



BAY 1129980 solution

S.3.1.80-01

Structure Elucidation - Summary of Biochemical Characterization

Signatures:

content approved : Tiemann Frank (sgryu) 2014-02-14 15:41:59

content approved : Geisen Karl (phgei) 2014-02-17 10:59:00

document approved : Waggener John (mmaqh) 2014-02-17 22:00:05

valid since: 2014-02-17

S.3.1.80#008042441
DCTM-version: 1.0

Table of Contents

Structure Elucidation - Summary of Biochemical Characterization.....	3
1. Introduction.....	3
2. Methods Describing the Primary Structure of the Molecule.....	8
2.1 Amino Acid Analysis	8
2.2 N-terminal Sequence Analysis	9
2.3 Sequence Analysis of Light and Heavy Chain after Tryptic Digest	11
2.4 C-terminal Sequence Analysis	12
2.5 Tryptic Peptide Mapping	12
2.6 Identification of Drug Attachment Sites in BAY 1129980.....	14
3. Method Describing the Conformational Structure of the Molecule	21
3.1 SDS Polyacrylamide Gel Electrophoresis	21
3.2 Isoelectric Focusing (IEF)	24
3.3 Two-Dimensional Gel Electrophoresis (2-DE)	25
3.4 Immunoblotting	28
3.5 Reversed Phase HPLC Chromatography and UV-Spectrum	29
3.6 Separation of Light and Heavy Chains.....	36
3.7 Capillary Zone Electrophoresis	39
3.8 Size Exclusion Chromatography	39
3.9 Ion-Exchange Chromatography.....	40
3.10 Molecular Weight Determination by HPLC-MS	43
4. Methods Dealing with Protein Bound Carbohydrates	45
4.1 Lectinblotting	45
4.2 Sialic Acid Determination	46
4.3 Monosaccharide Determination.....	48
4.4 Oligosaccharide Profile Analysis	49
5. Methods Dealing with the in Vitro Biological Activity of the Molecule	50
5.1 Determination of the Kinetic Constants of Interaction with the Antigen C4.4a	50
5.2 Affinity Blot of BAY 1129980 with the C4.4a Antigen	52
6. List of Abbreviations	53

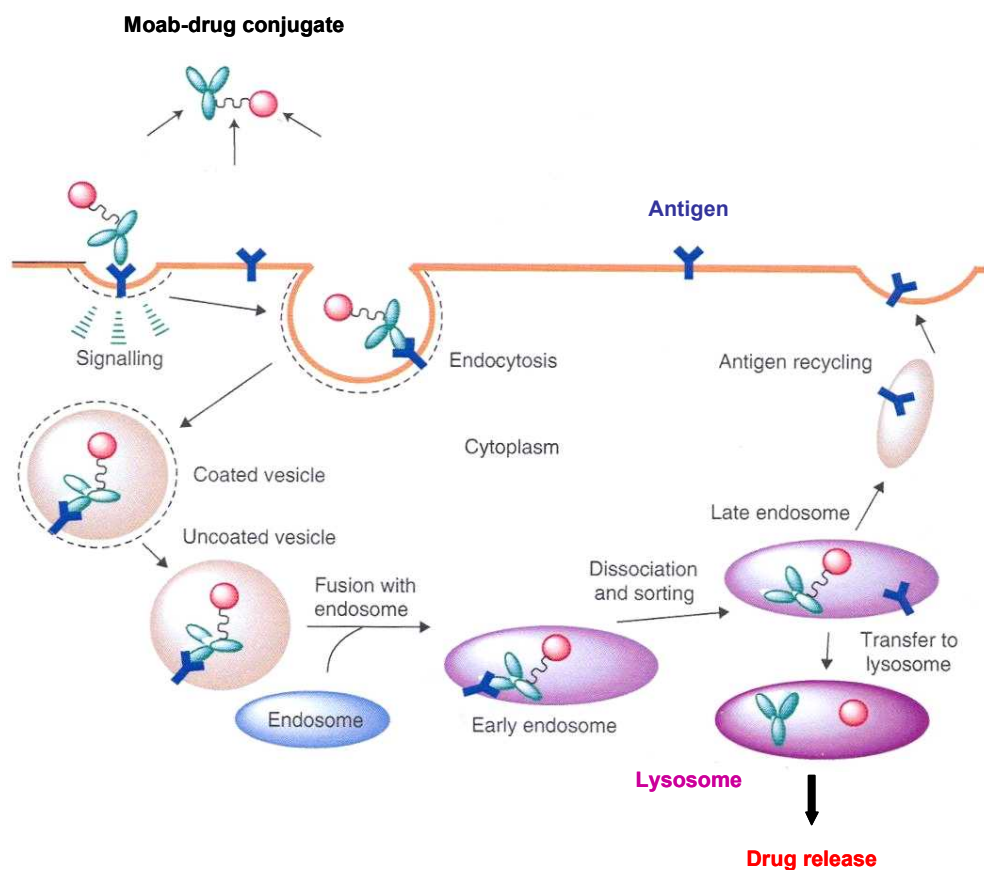
Structure Elucidation - Summary of Biochemical Characterization

1. Introduction

Cancer is the second leading cause of death in the developed countries and remains one of the most challenging diseases for physicians. One of the major reasons for difficulty in cancer treatment is that cancer cells originate from the host. Traditional chemotherapeutic agents lack the specificity required to kill tumor cells without simultaneously damaging healthy tissue and thus causing severe side effects. In order to solve the tumor-specificity problem associated with chemotherapeutic agents prodrugs could be constructed built up of the cytotoxic agent and a tumor targeting molecule. This prodrug is delivered to malignant tissue cells and internalized to release the cytotoxic agent to kill the cancer cells.

The discovery of antigens that are particularly overexpressed on a cancer cell membrane and the first description of monoclonal antibodies possessing high binding to tumor specific antigens opened a new area for the development of mAb based tumor–targeting chemotherapy.

The mAb-based immunoconjugate consists of three parts the monoclonal antibody, the cytotoxic agent and an appropriate linker. The monoclonal antibody is the vehicle that carries the conjugate to the target site. Currently, the most widely used antibodies are of the human IgG type. [Figure 1-1](#) shows the mechanism of action of the antibody based drug.

Figure 1-1. Mechanism of Action of the Antibody Based Anti-cancer Drug (1).

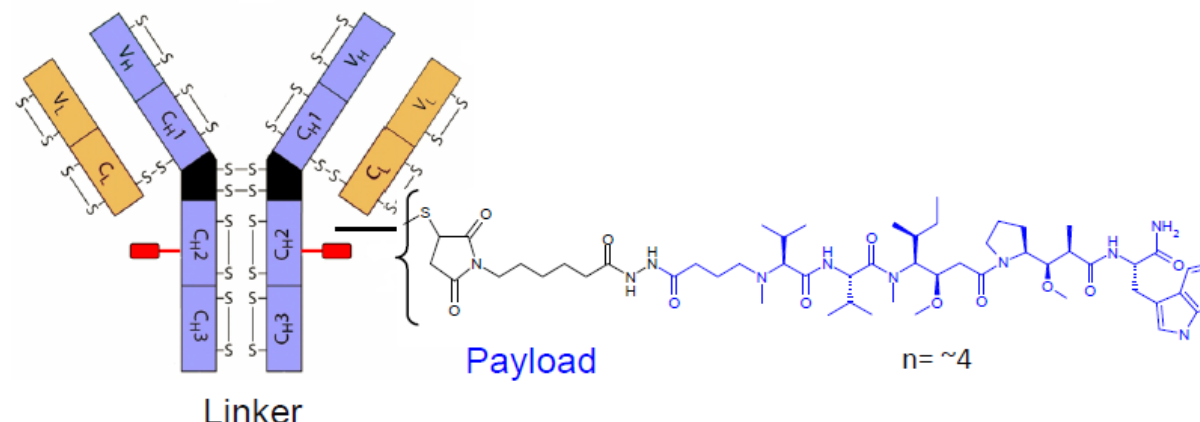
C4.4a is a structural homologue of the urokinase-type plasminogen activator (uPAR). It was originally identified as a metastasis-associated membrane protein and belongs to the GPI-linked protein family (2).

The GPI-anchor is responsible for fixing the protein in the plasma membrane. Mature C4.4a contains two uPAR / Ly6 domains and a Ser/Thr/Pro-rich (STP) region that includes a protease sensitive site. Mouse C4.4a shares 80% and 92% amino acid sequence identity with human and rat C4.4a, respectively.

C4.4a is a molecule of variable length (~65-100 kD) with cell type specific N-and O-linked glycosylation. Proteolytical cleavage following the second uPAR/Ly6 domain generates a 35-40 kD soluble form while ADAM10 or ADAM17 mediated cleavage within the STP region generates a 90 kD soluble form. Soluble C4.4a can also be shed and released in membrane vesicles. It is expressed in the suprabasal layers of stratified squamous epithelium and is upregulated on migrating keratinocytes during wound healing. Its expression is downregulated during the onset of epithelial dysplasia but subsequently up-regulated at the invasive front of melanomas and various carcinomas (2). Metastases derived from these tumors also express high levels of C4.4a. C4.4a over-expression in non-small cell lung cancer is predictive of increased mortality (3). Due to these facts, C4.4a is a potential target for intervention in cancer.

BAY 1129980 is an antibody-drug conjugate (ADC) which is built up of the monoclonal antibody BAY 1112623 directed against the C4.4a-antigen and a non-cleavable hydrazide linker combined with the auristatin-based tubulin inhibitor for taxane sensitive tumors (payload). [Figure 1-2](#) gives a schematic view of the drug.

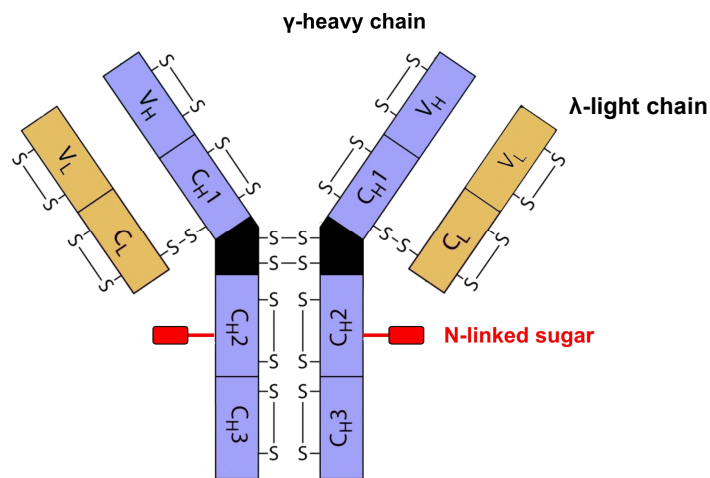
Figure 1-2. A Schematic View of the Antibody Conjugate BAY 1129980



The monoclonal antibody BAY 1112623 is one of the key components of the drug. It binds with high affinity to human C4.4a. BAY 1112623 is produced by fermentation of a recombinant CHO-cell as fed batch culture.

It belongs to the IgG1 subclass and consists of two identical lambda light (L) and two gamma heavy (H) chains which are connected via disulfide bonds. The molecule is divided into homologous regions of sequence, each of which has an intra-chain disulfide bridge. VH and VL represent the hypervariable regions that in the three-dimensional structure together form the antigen-binding site. N-linked carbohydrate moieties are attached to a conserved position at Asn(297) of the heavy chains in the CH2-domains. The molecular weight of IgG1 molecules is in the range of about 150 kD. A schematic structure of the IgG1 molecule is given in [Figure 1-3](#).

Figure 1-3. Schematic Representation of the IgG1-Molecule. The polypeptide chains, single domains, glycan attachment sites and SS-cross-links are shown. The light chains contain 217 and the heavy chains 450 amino acid residues each in case of BAY 1129980.



Conjugation with the drug-linker construct is achieved by first reducing the inter-chain disulfide bonds (four) of the mAb by e.g. TCEP. These SS-bonds are clustered in a highly flexible region of the mAb and therefore are much more accessible for reducing agents than the intra-chain bonds (twelve). The reduction proceeds through various pathways and produces a mixture of mAb species composed of 2, 4, 6 or 8 cysteines. The conjugation of the drug-linker construct follows a standard protocol based on the Michael-addition of the cysteine sulfhydryl groups of the mAb to the maleimide moiety of the drug-linker conjugate (Figure 1-4). Normally, a mixture of conjugates is generated ranging from two up to eight drugs per antibody depending on the reduction state of the mAb. Furthermore, partial reduction is also responsible for position isomers of BAY 1129980. Figure 1-5 shows the positions of possible drug-isomers which can be formed depending on the reduction state of the mAb.

Figure 1-4. Reaction of the maleimide toxophore derivative with the reduced mAb.

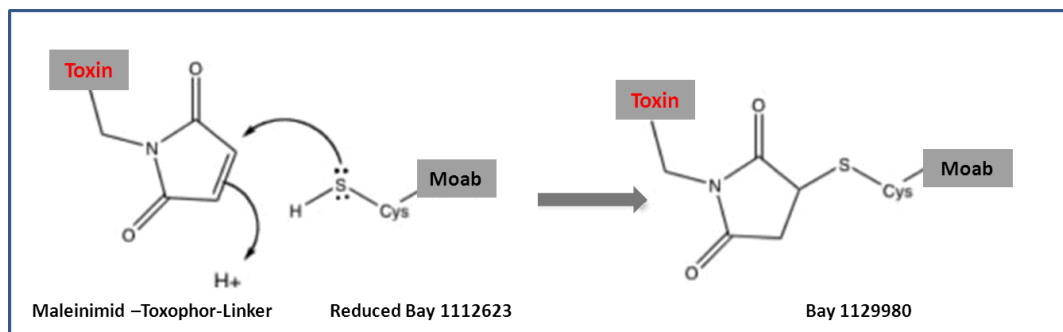
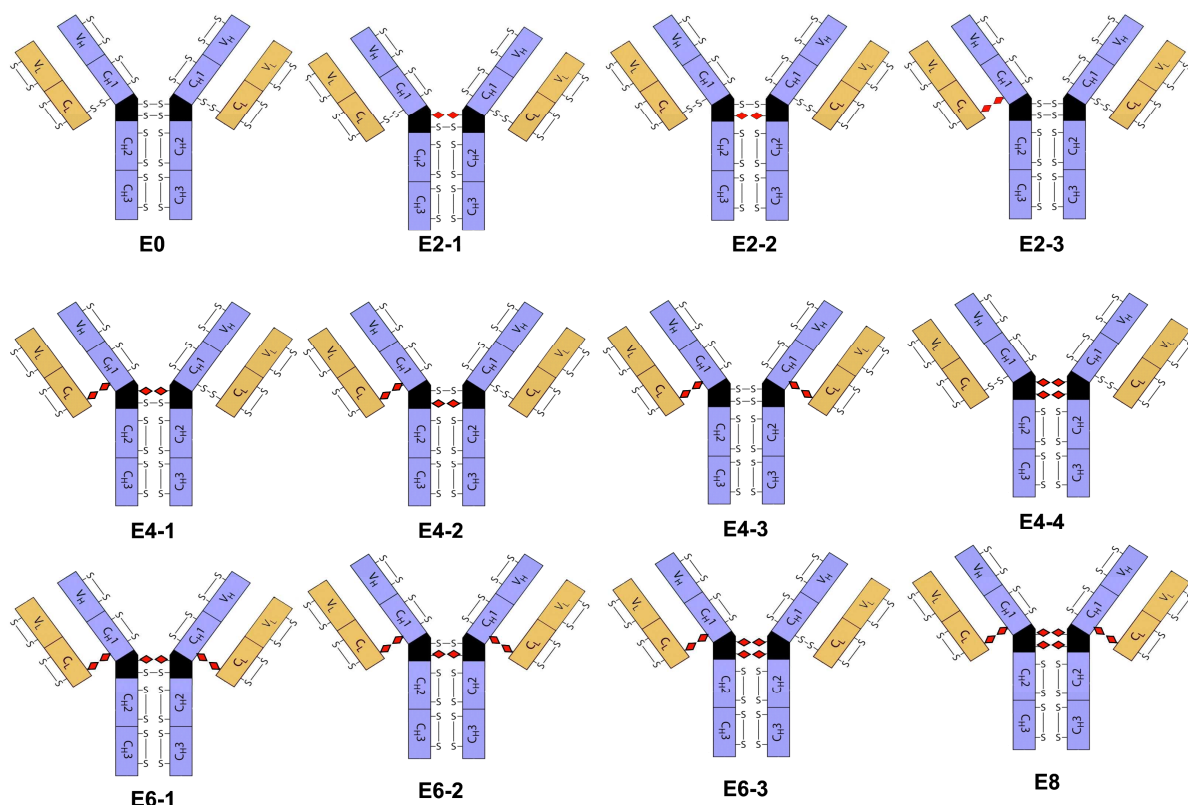


Figure 1-5. Schematic Representation of the Possible Conjugate Species after Reduction of Inter-chain Disulfide Bonds. Partial reduction can lead to several position isomers. E0 represents the non-conjugated form.



This report describes the protein chemical characterization of the BAY 1129980 solution batch BXR5PKW in comparison with the non-conjugated mAb (BAY 1112623, also referred to as X2213). The comparison of both the conjugated and the non-conjugated antibody shows the influence of the conjugation process to the protein. BXR5PKW will be used for preparation of the reference standard and for toxicological studies.

Detailed physico-chemical analysis using a variety of different techniques was performed to characterize the BAY 1129980 solution GLP-batch that will be used for preclinical activities like toxicological purposes, reference standard generation or pharmacokinetic analyses. The methods applied address different physico-chemical properties, such as conformational structure and post-translational modifications of the molecule to show the consistency and purity. The analyses used are e.g.: amino acid analysis, N-terminal sequence analysis, peptide mapping, SDS-gel electrophoresis, isoelectric focusing, reversed phase chromatography, separation of light and heavy chains, sialic acid determination, monosaccharide determination, analysis of toxophore binding sites, etc.

2. Methods Describing the Primary Structure of the Molecule

2.1 Amino Acid Analysis

Amino acid analysis is both a qualitative and a quantitative tool for the characterization of proteins. Information on the composition or identity, the incorporation of uncommon amino acids (e.g., N-methyl lysine) and the concentration of a protein solution are obtained. The protein must be first hydrolyzed to its constituent amino acids to perform the method.

All amino acids with the exception of tryptophan were determined, including cysteine as cysteic acid after performic acid oxidation. The discrimination between glutamine and glutamic acid as well as asparagine and aspartic acid is not possible due to the acid hydrolysis involved. The amino acids e.g., N-methyl valine, 6-aminohexanoic acid (6-AHA), Valine etc. from the drug-linker conjugate were also hydrolyzed. This allows the identification of the number of the conjugated toxophore. Table 1 shows a comparison of the amino acid analyses from C4.4a-ADC and C4.4a-mAb related to Asx=102 with the theoretical composition of the C4.4a antibody. The amino acids serine and threonine were not corrected for hydrolysis losses. The determined composition matches the theoretical numbers very well taking into account the limitations of the method. The hydrolysis losses are about 1%.

As expected for the conjugation the antibody-drug-conjugate contains less cysteic acid and some more valine than the mAb. Additionally, the uncommon amino acid 6-aminohexanoic acid was found. The number of about 3.5 6-AHA per mAb is in correspondence with the expected number of four toxophores/mAb designed by synthesis. Furthermore, this is in good correlation with HPLC-analysis and mass-spectroscopic investigation showing also about four drug-conjugates per mAb.

6-Aminohexanoic acid can only be completely released by prolonged standard hydrolysis (43h, 110°C) or by strong acid hydrolysis under higher temperature (1h, 166°C). The reason for slow release is probably the stability of the hydrazide bond and steric protection due to uncommon amino acids inside the toxophore. This is also the reason for the low valine numbers in the C4.4a-ADC during standard acid hydrolysis.

Table 2-1. Amino acid analyses of BAY 1112623 and BAY 1129980. The results are given in whole numbers related to Asx=102.

Amino Acid	Study No.		Theoretical Numbers
	mAb BAY 1112623	ADC BAY 1129980	mAb
CYSO3H ^a	29.14	27.15	32
ASX	102.00	102.00	102
THR	97.98	97.87	102
SER	156.93	157.72	174
GLX	113.99	113.81	114
GLY	100.04	99.40	98
ALA	85.87	85.06	82
VAL ^b	115.09	116.00	120 ^a
MET	8.42	9.06	8
ILE	25.40	25.24	26
LEU	104.74	104.42	104
TYR	55.78	55.64	56
PHE	35.99	35.86	36
HIS	24.27	25.82	24
6-AHA ^c	-	3.42	-
LYS	88.81	88.96	84
ARG	36.03	36.56	36
PRO ^a	100.39	101.81	100
TRP ^b	28.00	28.00	28 ^a
Sum AA	1308.85	1313.80	1326
hydrolysis losses in %	1.29	1.22	

^a Cys-SO₃H and Pro were from performic acid oxidation.

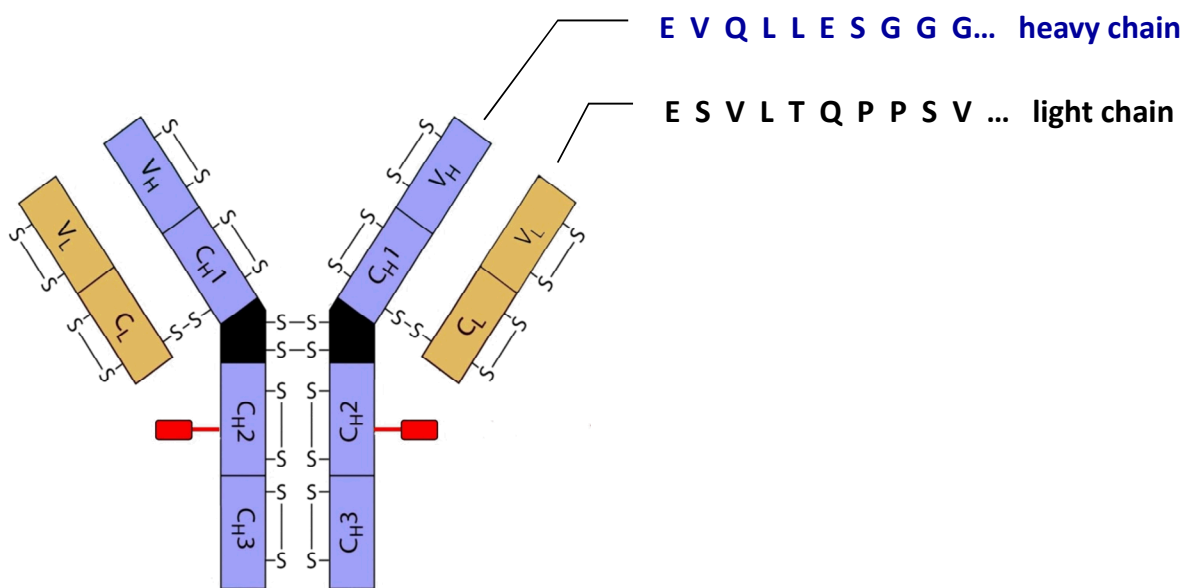
^b Trp and Val were from theoretical composition of mAb.

^c 6-AHA was determined by 1h 166°C hydrolysis.

2.2 N-terminal Sequence Analysis

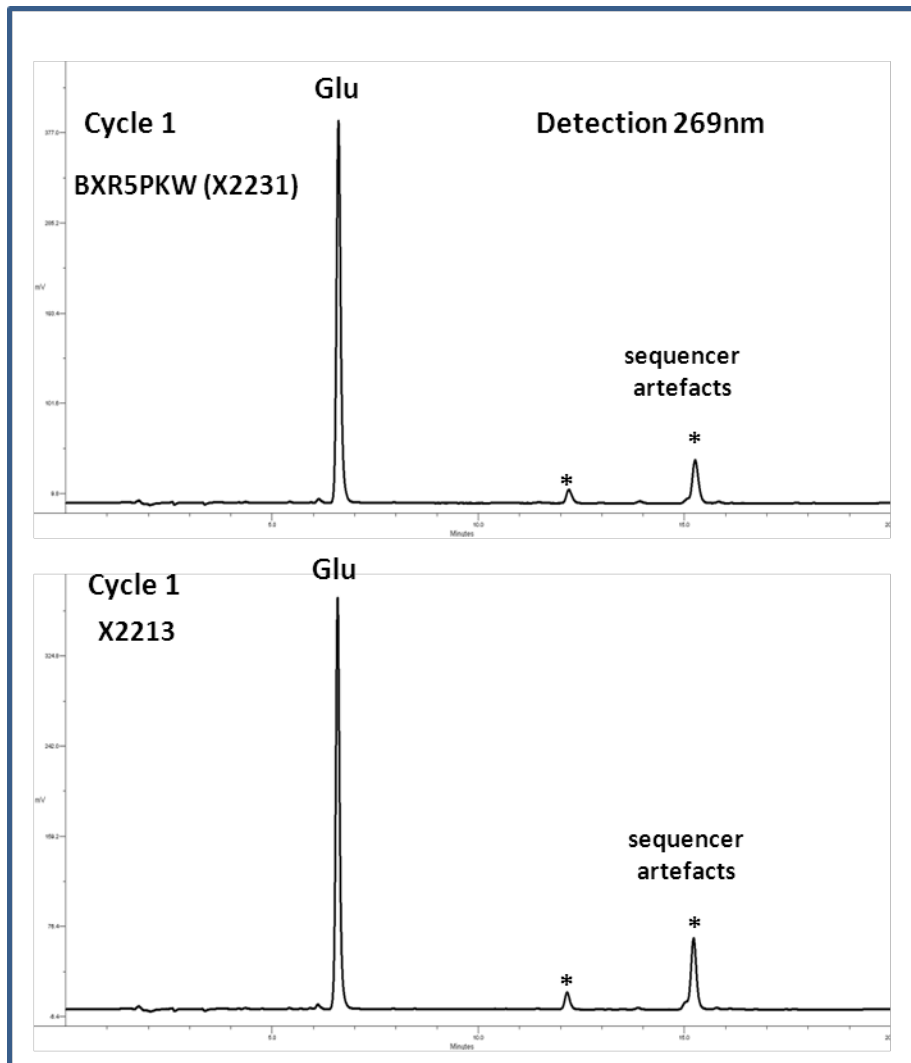
The monoclonal antibody BAY 1112623 belongs to the IgG1 subclass. The antibody consists of two identical gamma heavy chains (H) and two identical lambda light chains (L). As a result of the four chain structure two N-terminal sequences are to be expected if the entire molecule is sequenced. The same is valid for C4.4a-ADC. It was subjected to N-terminal sequence analysis over ten steps. The light and the heavy chain show no N-terminal blockage or other N-terminal microheterogeneities on the amino-terminus. One sequence was detected in the first cycle because of the N-terminal glutamic acid on both chains. In the following cycles two sequences were detected one coming from the light and one from the heavy chain. The sequences are in correspondence to the cloned amino acids of BAY 1112623. [Figure 2-1](#) shows the determined sequences and the amount of PTH-Glu in the first sequencer cycle representing the sum of PTH-Glu from light and heavy chain. [Figure 2-2](#) shows the HPLC-profiles of PTH amino acids from N-terminal sequence analyses of the first sequencer cycle from the ADC and the mAb. The conjugation process has no influence on the N-terminal sequences of the mAb and produces no chain cleavages.

Figure 2-1. N-terminal sequence analysis of BAY 1112623 GLP-batches. Study no., sequencer no., loaded amount and sum of PTH-Glu from light and heavy chain of the first sequencer cycle are given.



Study No.	Sequencer No.	Loaded Amount μg	% PTH- Glu
BAY 1112623 (mAb)	PRO 1364A	75	96
BAY 1129980 (ADC)	PRO 1364E	75	96

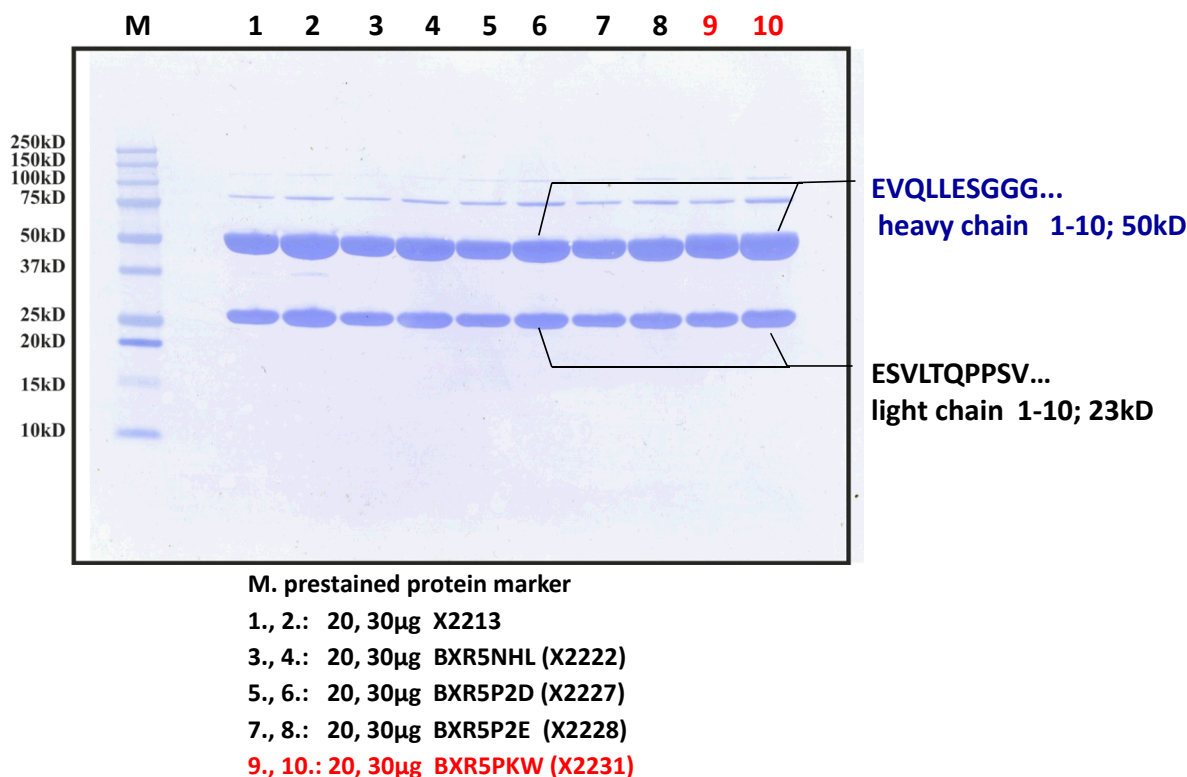
Figure 2-2. PTH-amino Acids of the First Sequencer Cycle from BAY 1129980 (BXR5PKW) and BAY 1122623



2.3 Sequence Analysis of Light and Heavy Chain after Tryptic Digest

Separation of light and heavy chains of BAY 1129980 was performed by SDS-gel electrophoresis under reducing conditions. The protein was then blotted onto a PVDF-membrane. Light and heavy chains of BAY 1129980 were directly sequenced from the membrane. The mAb batch BXR5P2D was also sequenced from this blot. The determined sequences and the blot are shown in [Figure 2-3](#). The sequences of light and heavy chain correspond to the cloned sequences of BAY 1112623. The conjugation process has no influence on the N-terminal sequences of light and heavy chain.

Figure 2-3. Westernblot of BAY 1129980 (BXR5PKW) and BAY 1112623 GLP-batches under Reducing Conditions. The proteins were separated by a 12% SDS-gel and then blotted onto a PVDF-membrane. The membrane was stained using Coomassie Blue Brilliant R-250. The sequenced bands are marked.



2.4 C-terminal Sequence Analysis

The C-terminus of BAY 1129980 was determined by HPLC-ESI-MS measurement of the reduced light and heavy chains. The correct masses of both chains could be confirmed indicating the correct C-terminus of light and heavy chain.

2.5 Tryptic Peptide Mapping

For the fragmentation of the BAY 1112623 an enzymatic method based on the enzyme trypsin was used. This proteinase cleaves peptide bonds C-terminally of arginine and lysine. Trypsin is commercially available in a very consistently pure quality which is very important for getting reproducible peptide maps of proteins. Reverse-phase high pressure liquid chromatography (HPLC) has proved to be an extremely versatile technique for rapid separation of peptides. The excellent resolving power of HPLC enables separation of the majority of peptides within a mixture. HPLC offers the advantages of high reproducibility, easy quantitation, rapid analysis time, and it is suitable for automation.

BAY 1129980 was analyzed by tryptic peptide mapping in comparison with the C4.4a mAb batch BXR5P2D to see the influence of conjugation. The generated peptides were separated by HPLC and analyzed for retention times of selected peaks at three different wavelength

210nm, 280nm and 295nm. BAY 1129980 and BAY 1112623 samples are highly comparable with respect to peak number and peak position at 210 nm, 280 nm and 295 nm ([Figure 2-4](#), [Figure 2-5](#) and [Figure 2-6](#)). There are only some minor additional peaks which are most probably coming from the drug-linker. The reason for the high similarity of the tryptic peptide maps is most probably a retro reaction of the conjugate under the high pH at elevated temperature used for tryptic peptide mapping. These conditions are necessary for reductive carboxymethylation before tryptic cleavage. In summary, comparative peptide mapping of BAY 1129980 and BAY 1112623 show nearly identical profiles indicating that the same primary structure and posttranslational modifications were practically not changed by the conjugation process.

Figure 2-4. Overlay of HPLC-profiles of the Tryptic Peptide Map of BXR5PKW (BAY 1129980) and BXR5P2D at 210 nm. The conservative glycan peptide is marked.

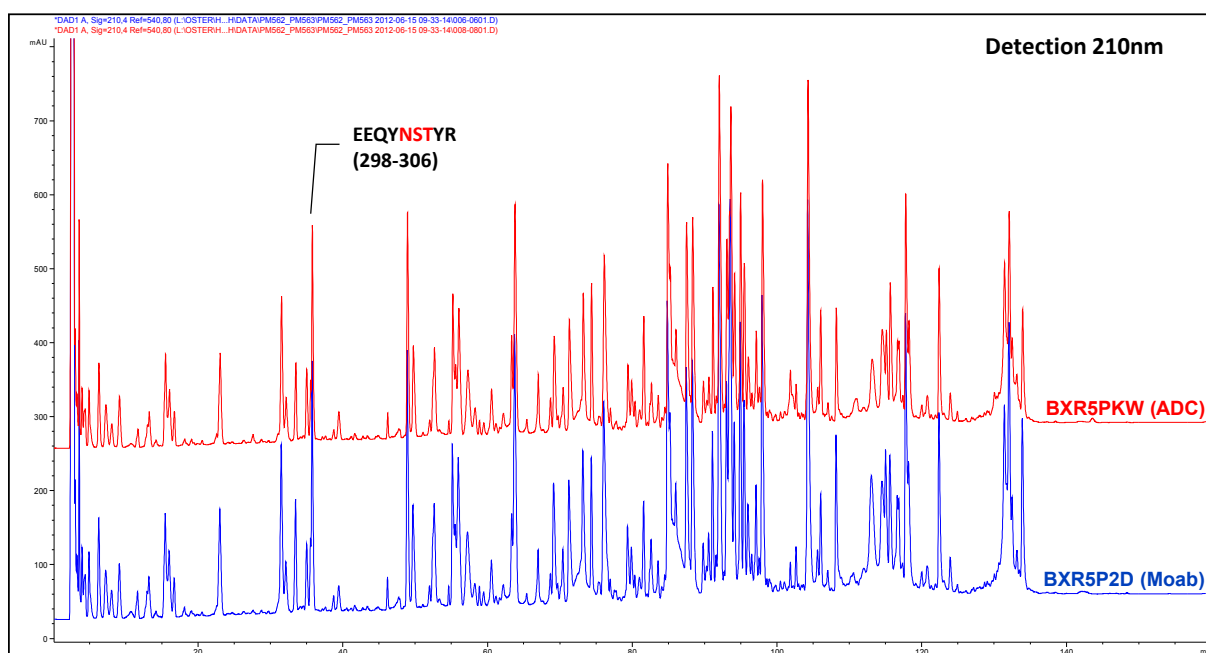


Figure 2-5. Overlay of HPLC-profiles of the Tryptic Peptide Map of BXR5PKW (BAY 1129980) and BXR5P2D at 210 nm. The conservative glycan peptide is marked.

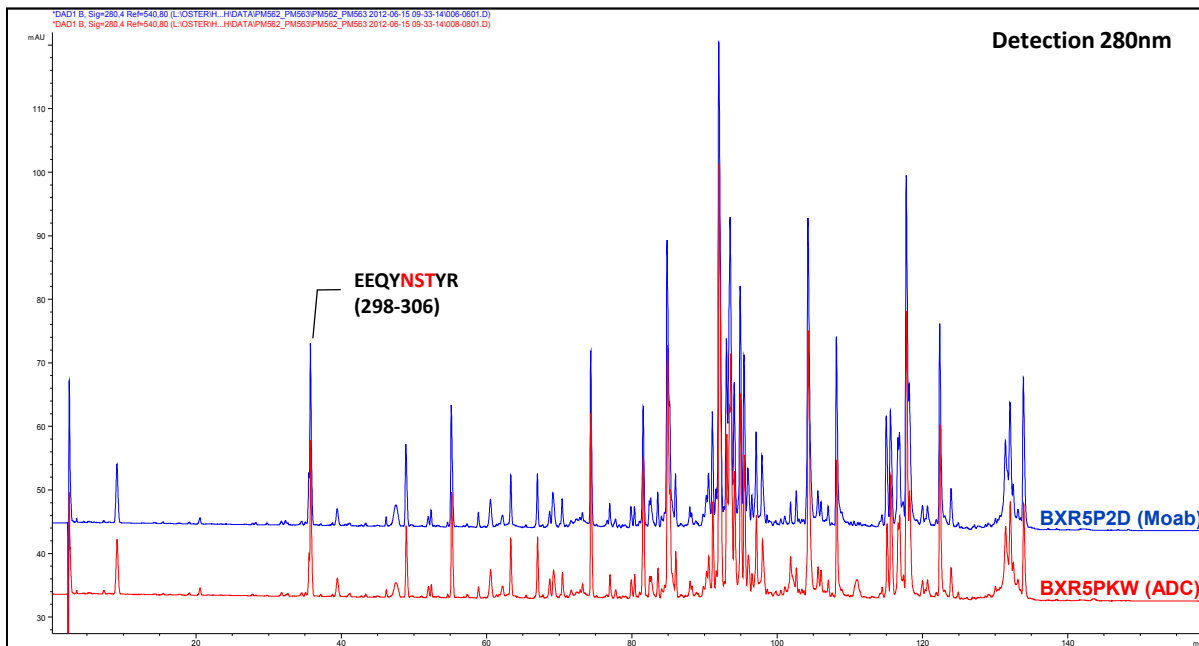
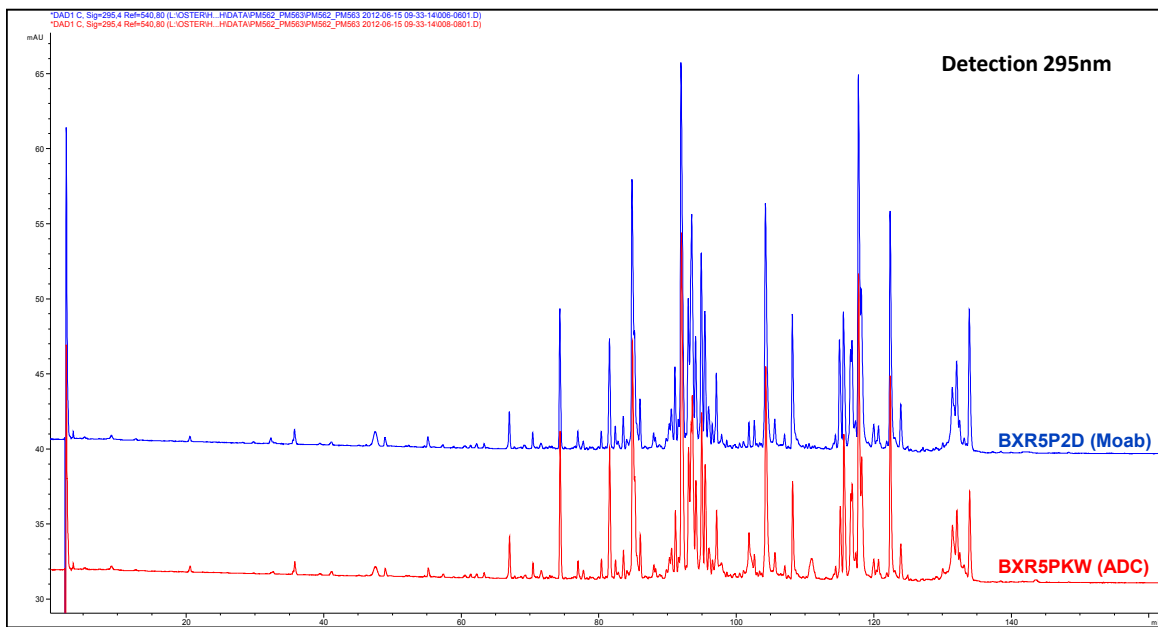


Figure 2-6. Overlay of HPLC-profiles of the Tryptic Peptide Map of BXR5PKW (BAY 1129980) and BXR5P2D at 295 nm



2.6 Identification of Drug Attachment Sites in BAY 1129980

Analytical peptide mapping using the non-specific metalloproteinase thermolysin was used to digest BAY 1129980 and BAY 1112623 under native conditions. The resulting peptide fragments were then separated by reversed-phase HPLC. Thermolysin is able to cleave at

about pH 6, which means that disulfide shuffling is avoided during cleavage. The thermostable endopeptidase thermolysin from *Bacillus thermoproteolyticus* has a broad specificity for the N-terminal side of hydrophobic residues, particularly leucine, isoleucine, phenylalanine, valine and methionine in descending order of preference (9). Therefore a large number of short peptides are normally generated. The exposure of sample proteins to basic pH conditions must be strictly avoided because the protein disulfide bridges are often rearranged at pH values higher than pH 8. Furthermore, the retro Michael type reaction and exchange reactions with internal cysteines/cystines of the mAb are increased at higher pH.

The rearrangement usually occurs via the nucleophilic attack of a thiolate anion ($-S^-$) to a sulfur atom of another disulfide bond ($-SS-$) with a single step SN₂ mechanism or to the succinimide thioether of the linker-toxophore group. The S^- anion can be generated at a pH above the pKa value of the thiol group (typically \sim pH 8.3).

The ADC was digested by thermolysin under native conditions to preserve SS-linkages inside the molecule and to preserve the succinimide thioether bond of the linker. The generated peptides were separated by HPLC and analyzed by overlaying the chromatographic profiles at different wavelengths. Furthermore, the UV-spectra of the individual peptides were carefully analyzed for identification of the linker-toxophore structure. The linker-toxophore-molecule contains a tryptophanamide which shows a characteristic UV-spectrum with absorption at about 295 nm. Additionally, the linker-toxophore residue is very hydrophobic dominating the properties of a short thermolytic peptide.

[Figure 2-7](#) shows an overlay of the thermolytic digests from ADC GLP-batch BAY 1129980 in comparison with the non-conjugated antibody (BXR5P2D). Two separate peptide groups can be observed in the BAY 1129980 digest in comparison with the non-conjugated antibody. The conjugated peptides also absorb at 295 nm as expected. The area percent of the conjugated peptides is about 7%.

[Figure 2-9](#) shows a HPLC-run of BAY 1129980 with a higher acetonitrile concentration. The toxophore carrying peptides are separated from the non-conjugated ones which are running with the breakthrough. This run was used for preparative separation of conjugated peptides. The non-conjugated antibody shows no peptides in this region (data not shown).

The toxin-containing peptides were preparatively isolated by fractionation ([Figure 2-8](#)) and then identified by protein sequencing and MS-measurement. The identified peptides are shown in [Table 2-2](#).

The PTH-amino acid cysteine-linker-toxin shows no UV-signal during Edman degradation and was identified by its absence. Careful analyses of the UV-spectra of numbered peaks show that all of the hydrophobic peptides (except for residual thermolysin) carry a toxophore residue. Examples of UV-spectra are given in [Figure 2-10](#). The non-conjugated peptides are very similar between the naked and the conjugated antibody. [Figure 2-11](#) a and b show two examples of MS-measurements. The conjugation of BAY 1129980 is very site specific. Only the cysteine in position 216 of the light chain is conjugated and for the heavy chain only the hinge region cysteines position 220, 226 and 229 of the heavy chain are conjugated. Other conjugated cysteines were not found.

Figure 2-12 a and b show the primary structures of light and heavy chain of BAY 1129980. The conjugated cysteines are marked. **Figure 2-13** gives a scheme of an IgG-mAb. The positions of conjugated cysteines are shown.

Table 2-2. Identified Peptides from Preparative Separation of Toxin-containing Thermolytic Peptides from BAY 1129980. Sequencer run, peptide number, position inside the molecule, toxin identified by UV- and MALDI mass spectrometry and the determined sequences are given.

Sequence r run	Chain	Position	Determined Sequence (Edman degradation)	Toxin UV	Toxin MS	Position Cysteine
Pro1369E	LC	215-217	ECS	+	a	216
Pro1369F	HC	225-230	T ^C PPC ^P ...	+	a	226, 229
Pro1369D	HC	215-221	VEP(K)SCD	+	a	220
Pro1369B	HCHC	219-223	1. SCDKT...	+	+	220
		215-221	2. VEPK ^S CD (Peak 1)			220
Pro1369C	LC	215-217	1. ECS	+	+	216
	HC	225-228	2. T ^C PP... (Peak 2)			226
Pro1369A	HC	225-232	T ^C PPC ^P AP	+	b	226, 229 (Peak 3)

^a not measured by MS

^b A MALDI spectra could not be measured.

Figure 2-7. Overlay of thermolytic Peptide Maps of BAY 1129980 (BXR5PKW) and BAY 1112623 (BXR5P2D) at 210 nm. The position of residual thermolysin and peaks from sample preparation are marked.

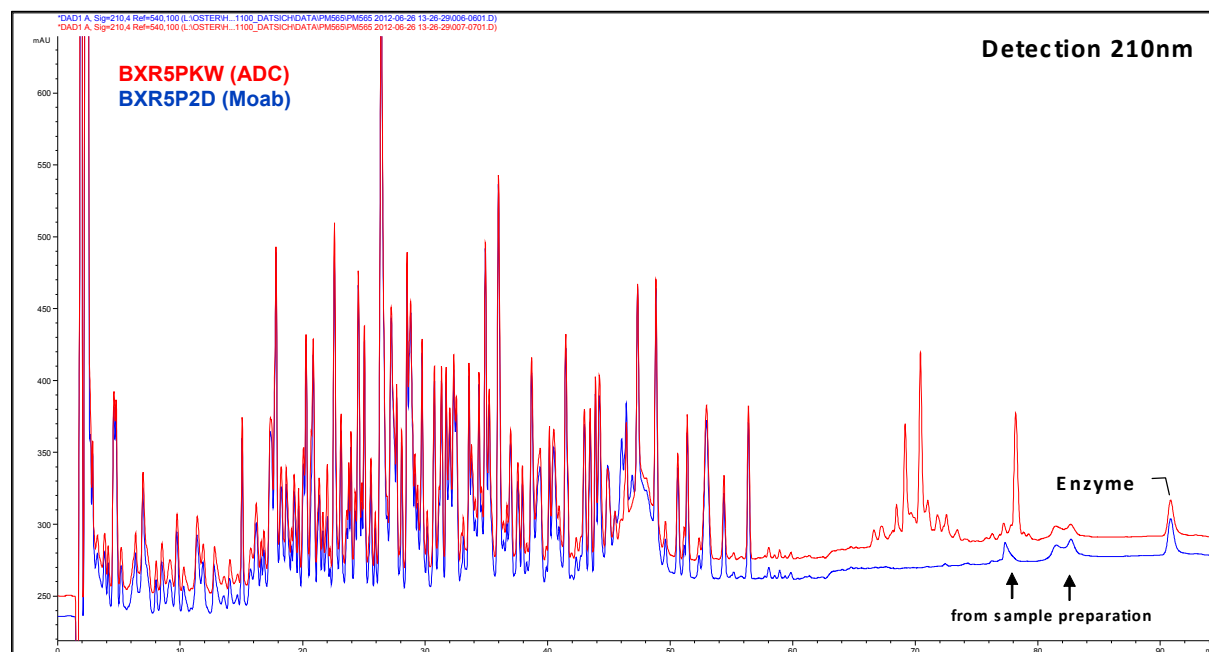


Figure 2-8. Preparative Thermolytic Peptide Map of BAY 1129980 at 210 nm. Peaks that were sequenced are shown..

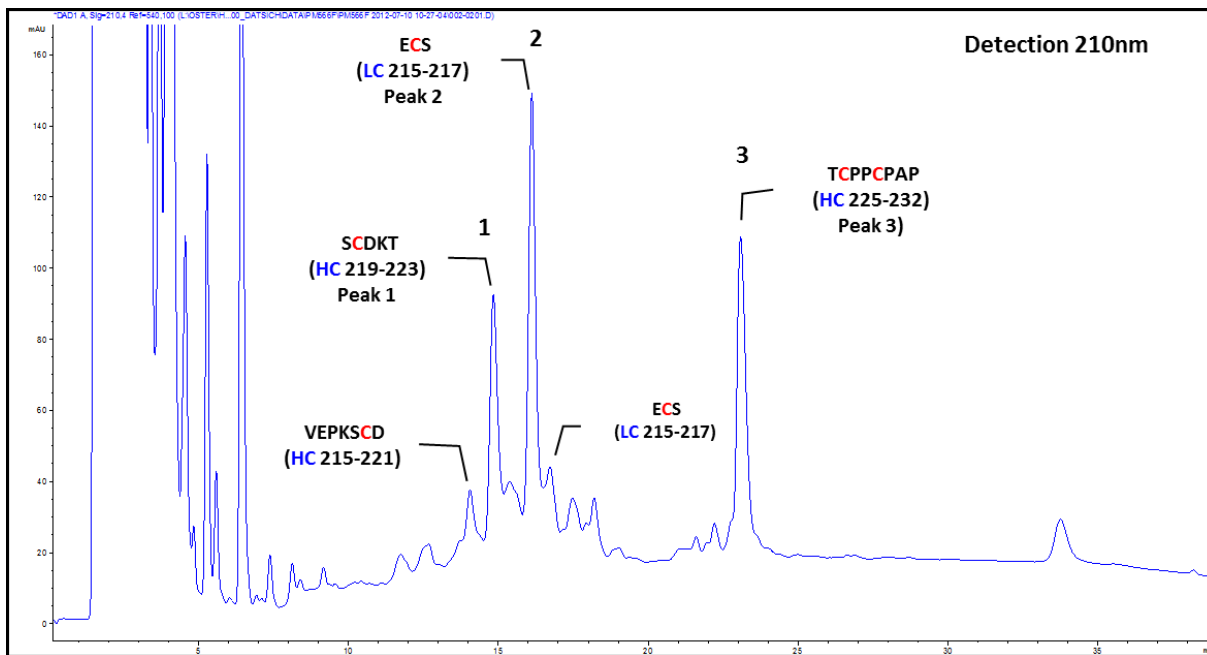


Figure 2-9. Preparative Thermolytic Peptide Map of BAY 1129980 at Three Different Wavelengths 210, 280 and 295 nm

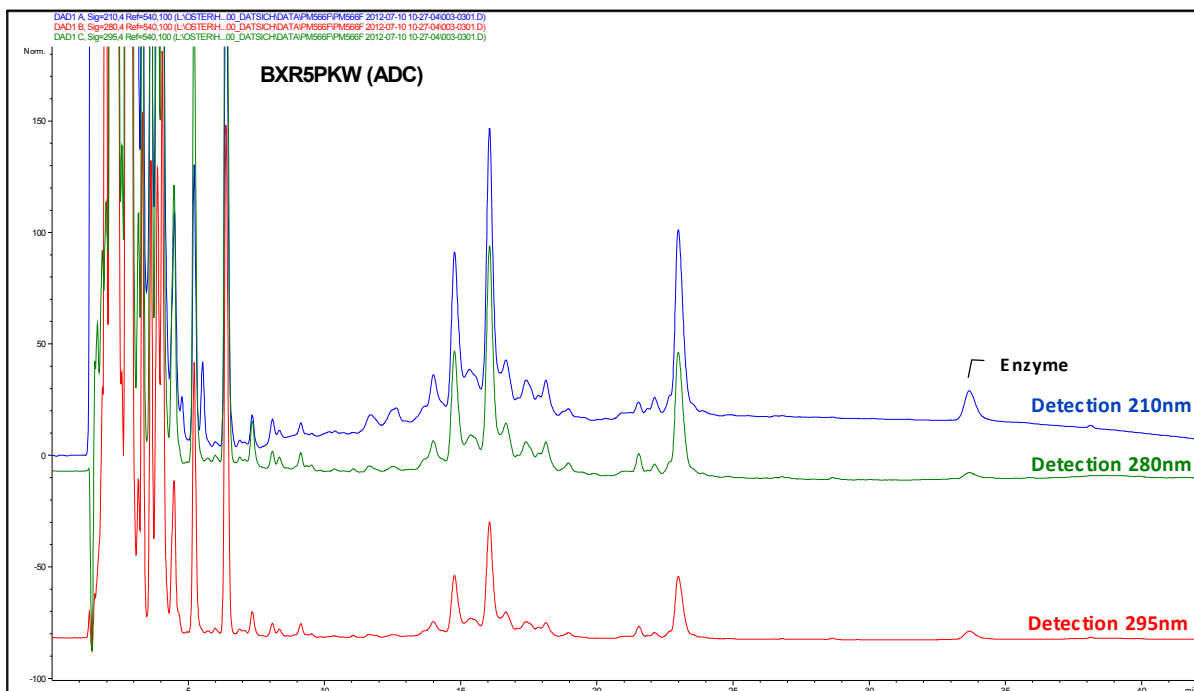


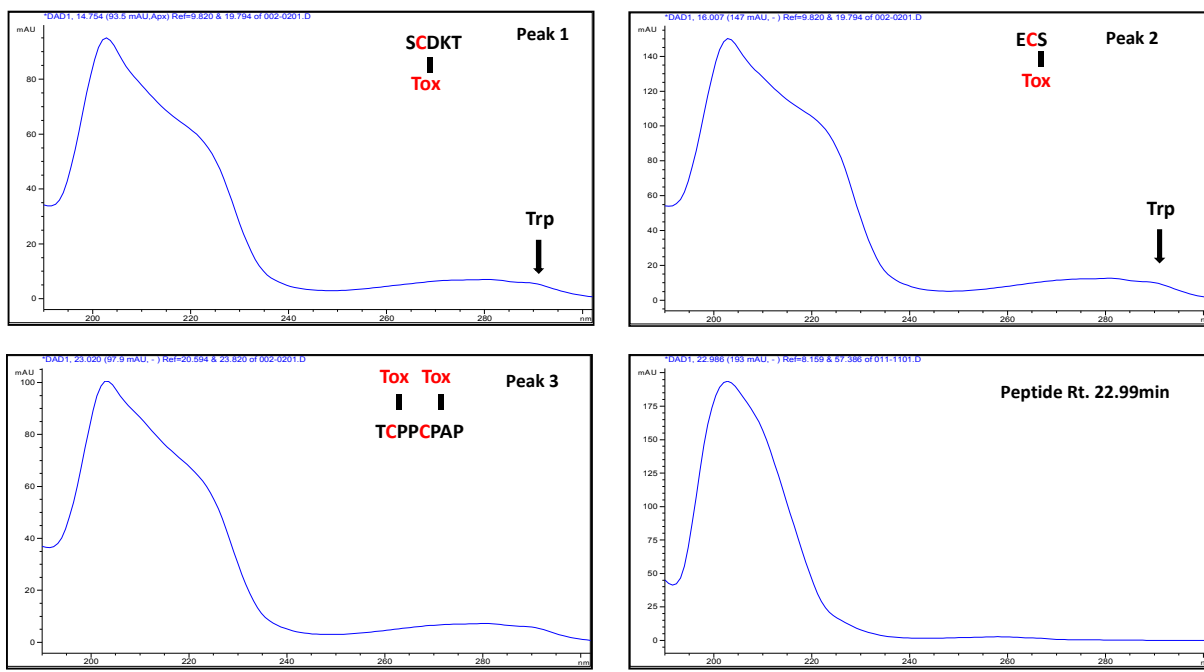
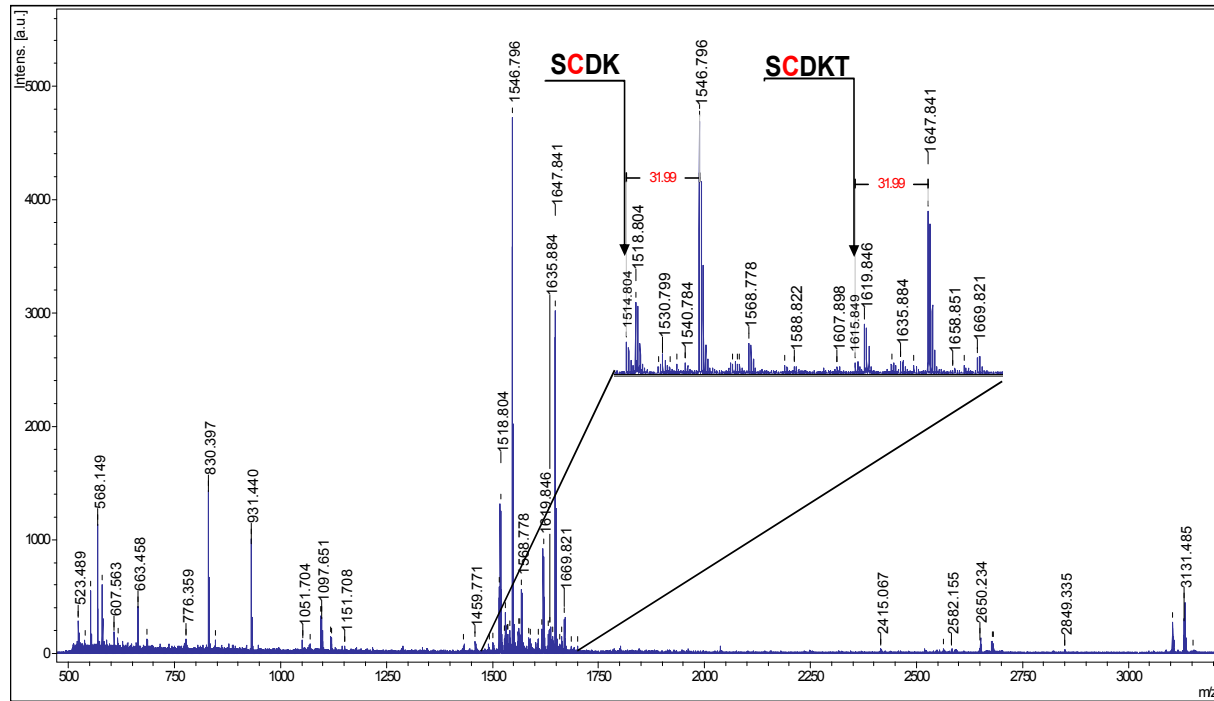
Figure 2-10. UV-spectra of Three Conjugated Thermolytic Peptides of BAY 1129980 in Comparison with a Non-conjugated One

Figure 2-11. MALDI Spectra of Peak 1 and Peak 2 of Thermolytic Peptide Map from BAY 1129980. The conjugated peptides are marked. An oxidized form is present from each peptide in addition to the original conjugated one.

a.



b.

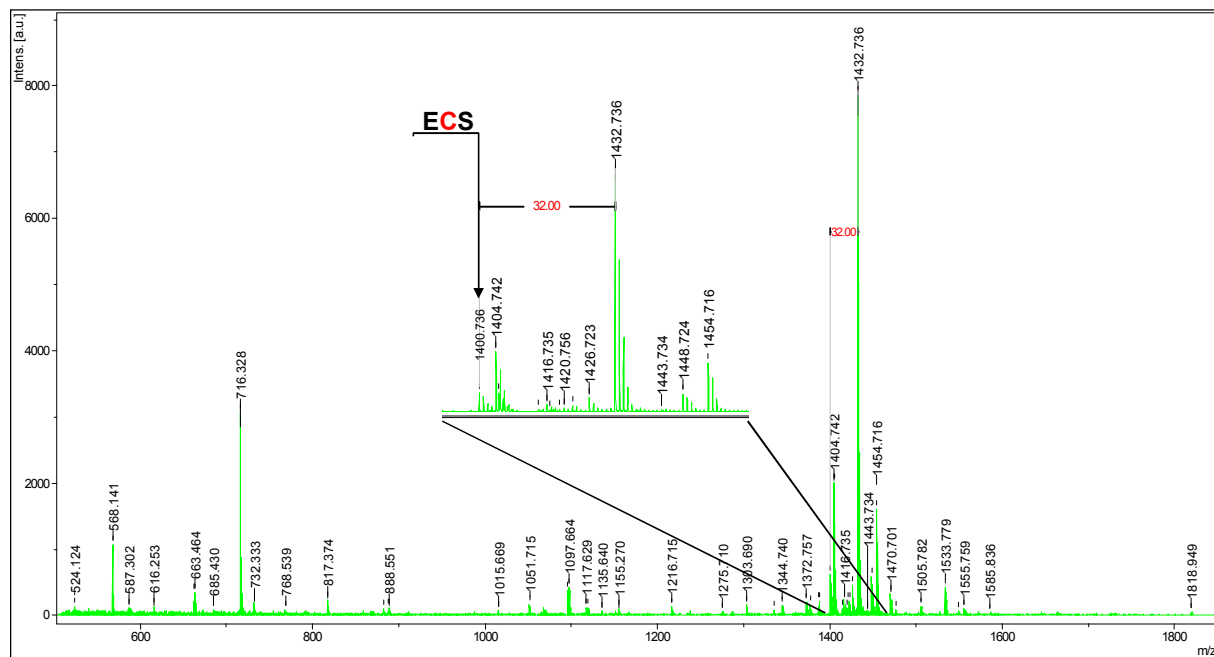


Figure 2-12. Primary Structure of Light And Heavy Chain of BAY 1129980. The conjugated peptides are marked.

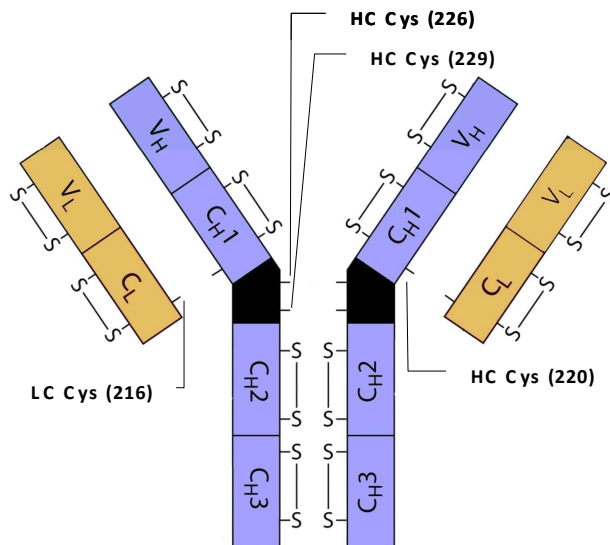
a.

ESVLTQPPSV SGAPGQRVTI S **C**TGSSSNIG AGYVVHWYQQ
LPGTAPKLLI YDNNKRPSGV PDRFSGSKSG TSASLAISGL
RSEDEADYY**C** AAWDDRLNGP FGGGTKLTVL GQPKAAPSVT
LFPPSSEELQ ANKATLV**C**LI SDFYPGAVTV AWKADSSPVK
AGVETTPSK QSNNKYAAS SYLSLTPEQW KSHRSYS**C**QV
THEGSTVEKT VAPTECS **Light chain**

b.

EVQLLESGGG LVQPGGSLRL S **C**AASGFTFS NAWMSWVRQA
PGKGLEWVSY I S S G S T I Y Y ADSVKGRFTI S RDNSKNTLY LQMNSLRAED
TAVYY**C**AREG LWAFDYWGQG TLTVSSAST KGPSVFPLAP SSKSTSGGTA
ALG**C**LVKDYF PEPVTWSWNSGALTSGVHTF PAVLQSSGLY SLSSVVTVP
SSLGTQTY**C** NVNHKPSNTK VDKKVEPKSC DKTHTCPPCP **A**PELLGGPSV
FLFPPKPKDT LMISRTPEVT **C**VVVVDVS HED PEVKFNWYVD GVEVHNAKTK
PREEQYNSTY RVVSVLTVLH QDWLNGKEYK**C**KVSNKALPA PIEKTISKAK
GQPREPQVYT LPPSRDELTK NQVSLTC**L**VK GFYPSDIAVE WESNGQPENN
YKTPPPVLDSDGSFFLYSKL TVDKSRWQQG NVFS**C**SVMHE ALHNHYTQKS
LSLSPG **Heavy chain**

Figure 2-13. Scheme of a IgG1-mAb. The positions of conjugated cysteines are given.



3. Method Describing the Conformational Structure of the Molecule

3.1 SDS Polyacrylamide Gel Electrophoresis

BAY 1129980 represents a partially reduced conjugated antibody that basically consists of two heavy (H) and two light (L) chains plus drug-linker conjugates with a molecular weight of about 150 kD. BAY 1129980 was analyzed by SDS-gel electrophoresis under reducing and non-reducing conditions. Quantification of light and heavy antibody chains was performed on the reduced Coomassie Blue Brilliant R-250 stained gel by scanning the protein zones with a densitometer. The ratio of heavy/light chain and the molecular weights was determined. [Figure 3-1](#) shows a 4-12% SDS-gel of BAY 1129980 under non-reducing conditions in comparison with C4.4a-mAb batches. The gel was stained first using Coomassie Blue Brilliant R-250 and secondly by silver stain. The position of whole ADC (~150 kD) is marked. The C4.4a-mAb runs with the same molecular weight of about 150 kD. Heavy chain ADC-fragments have a slightly higher molecular weight in comparison to the bands of the naked mAb indicating conjugation of the heavy chain.

[Figure 3-2](#) shows a 12% SDS-gel under reducing conditions. The gel was stained first using Coomassie Blue Brilliant R-250 and secondly by silver stain. Light and heavy chains are clearly separated as distinct bands. The heavy chain of the conjugate runs slightly higher than the one from the mAb. The molecular weights determined from the Coomassie gel of heavy chain is about 53 kD and that of light chain is about 28 kD. The ratio of heavy/light chain of the ADC is 1.79 which is slight higher than that of BAY 1112623 GLP-batches ([Table 3-1](#)).

Table 3-1. Ratios of Heavy/Light Chains of BAY 1112623 and BAY 1129980 Solution-Batches Determined by scanning the Coomassie Blue Brilliant R-250 Stained Gel Run under Reducing Conditions. The ratios were formed from the peak areas of the gel bands.

Batch	Ratio Heavy/Light Chain
BXR5NHL (BAY 1112623)	1.63
BXR5P2D (BAY 1112623)	1.61
BXR5P2E (BAY 1112623)	1.61
BXR5PKW (BAY 1129980)	1.79

Figure 3-1. 4-12%-SDS-gel of BAY 1112623 and BAY 1129980 Solution-batches First Stained by Coomassie Blue Brilliant R-250 and Second by Silver Stain under Non-reducing Conditions

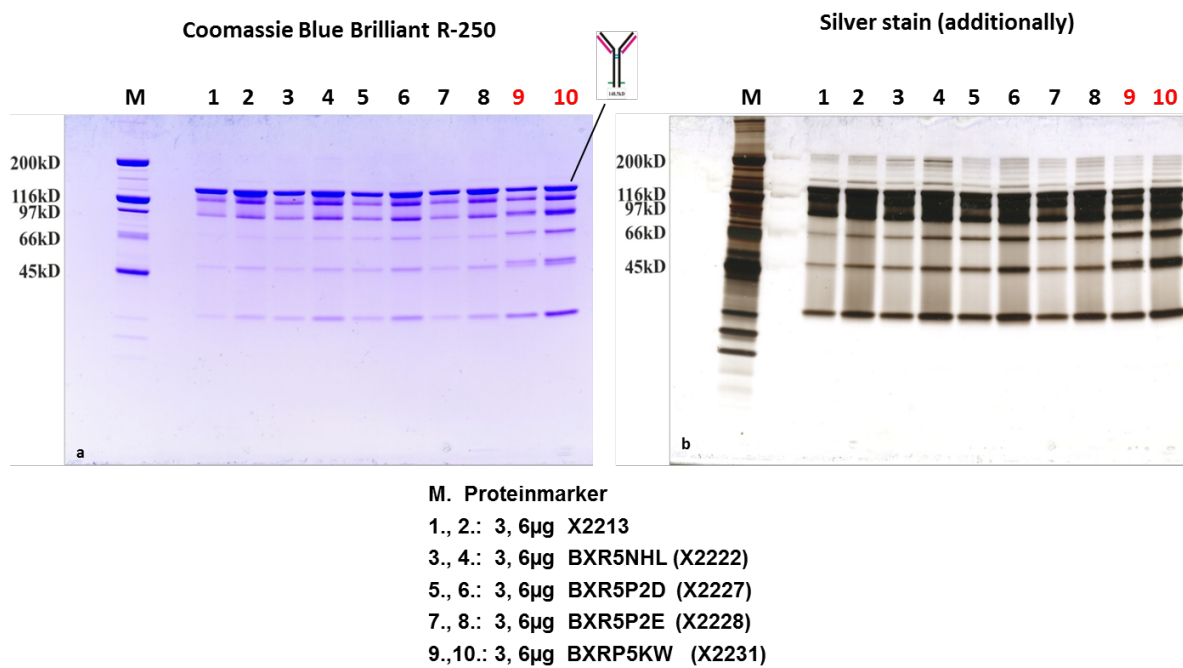
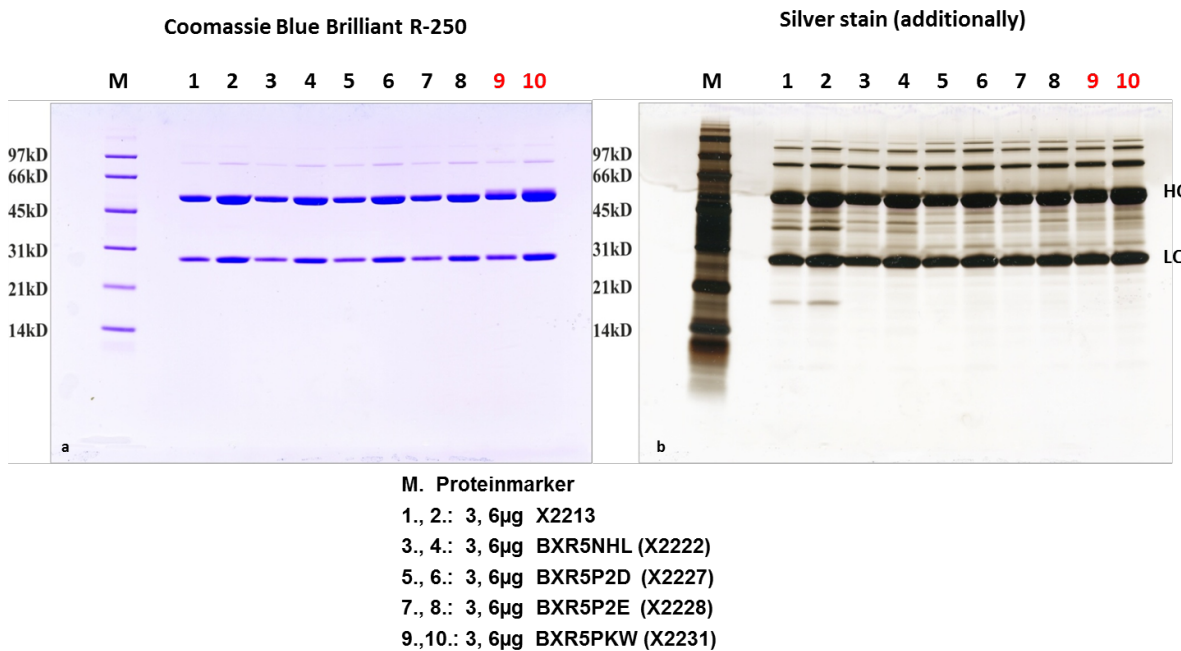
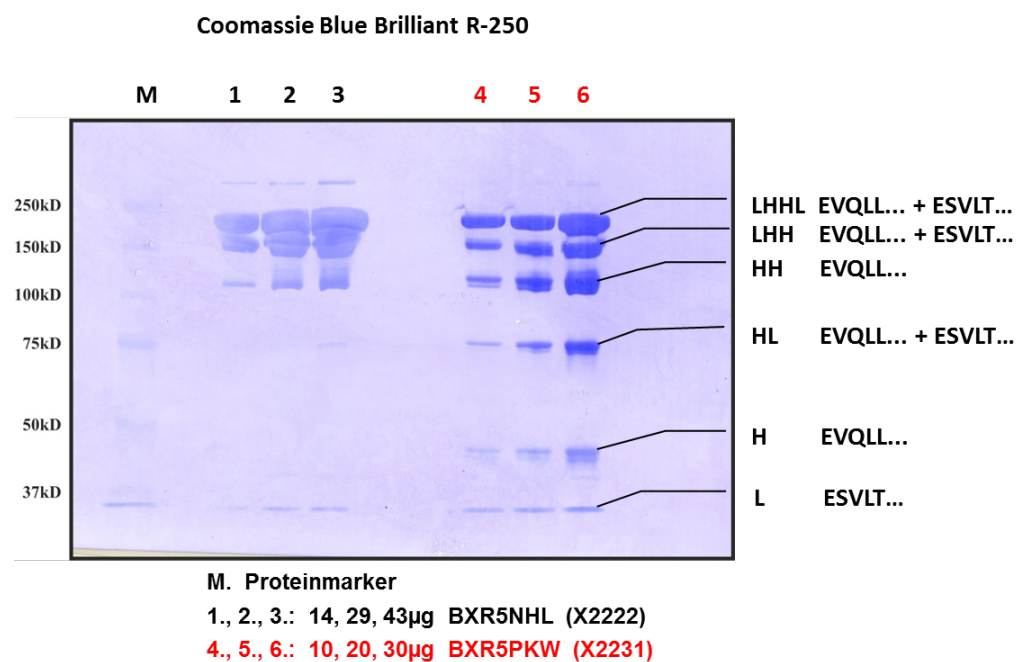


Figure 3-2. 12%-SDS-gel of BAY 1112623 and BAY 1129980-batches First Stained by Coomassie Blue Brilliant R-250 and Second by Silver Stain under Reducing Conditions



Separation of BAY 1129980 was performed by SDS-gel electrophoresis under non-reducing conditions. The protein was blotted onto a PVDF-membrane and single protein bands were directly sequenced from the membrane. The determined sequences and the assignment to the individual bands are shown on [Figure 3-3](#). The ADC is more fragmented than the naked mAb which comes from the conjugation process.

Figure 3-3. BAY 1129980 and the mAb were separated under non-reducing conditions by a 7.5% Tris-Glycine SDS-gel. The gel was blotted onto a PVDF-membrane, stained by Coomassie Blue Brilliant R-250. The single bands were N-terminally sequenced and the deduced structures are given.

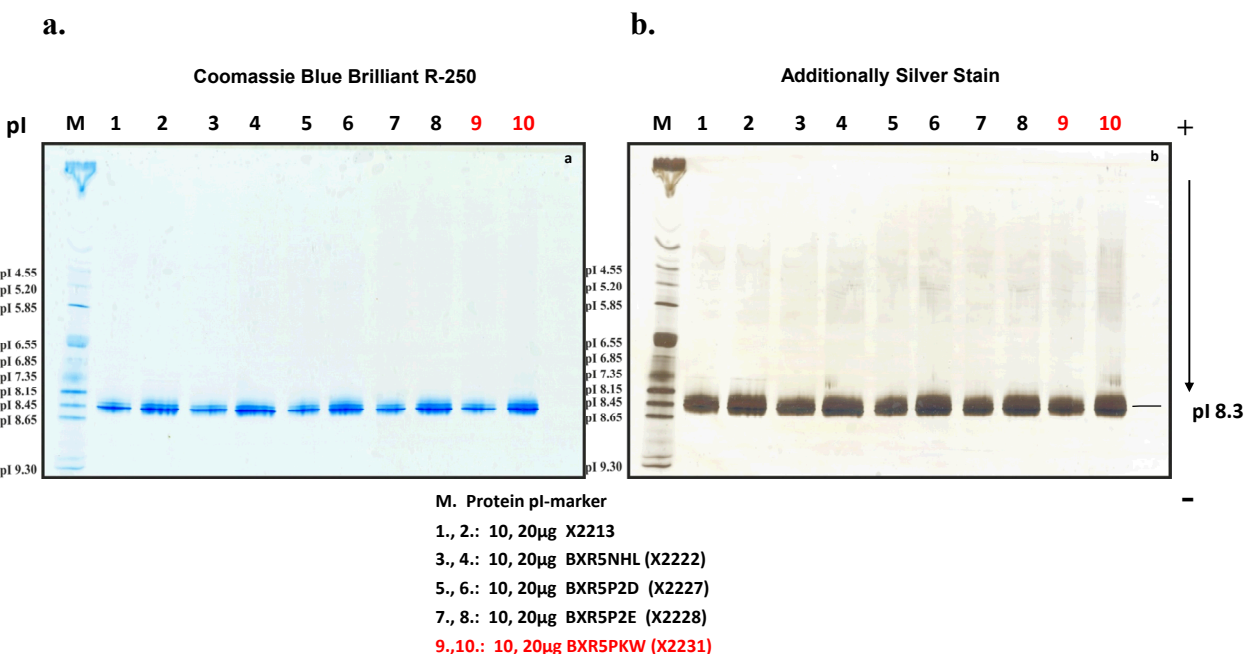


3.2 Isoelectric Focusing (IEF)

Isoelectric focusing (IEF) involves setting up a pH gradient and allowing the proteins to migrate in an electric field to the point in the system where the pH equals the isoelectric point.

BAY 1129980 was analyzed under non-reducing native conditions using isoelectric focusing. [Figure 3-4](#) (a and b) show the isoelectric focusing gel. The pH gradient used was mainly in the range of 3.5 up to 9.5. The gel was stained using Coomassie Blue Brilliant G-250 and additionally by silver stain. The Coomassie blue stained gel was also used for the determination of the isoelectric point of BAY 1129980 with the aid of an isoelectric focusing marker. The ADC shows several bands in a range from about pH 8.2 up to 8.4, with a main band (pI) of about 8.3. There is no difference between the mAb and the ADC in IEF running under non-reducing, non-denaturing conditions in a pH-range from about 3.5 up to 9.5. This behavior indicates that the antibody preserves its configuration under native conditions after conjugation.

Figure 3-4. Isoelectric focusing of BAY 1129980 and BAY 1112623 GLP-batches in the range of 3.5 up to 9.5 under non-reducing native conditions. The gel was stained by Coomassie Blue Brilliant G-250 and then additionally by silver stain.



3.3 Two-Dimensional Gel Electrophoresis (2-DE)

BAY 1129980 and BAY 1112623 were analyzed by 2D-electrophoresis under non-reducing conditions. The gels were stained by Coomassie Blue Brilliant G-250 or by silver stain. An IPG-gradient from 6 up to 11 was used for the first dimension. Figure 3-5 shows the 2D-gels of the BAY 1129980 and BXR5P2D under non-reducing conditions. BAY 1129980 is run as control in parallel without prior IEF in the SDS-gel (BAY 1129980 is only partially denaturized by SDS in case of non-reducing conditions). BAY 1129980 is separated according to its pI in the first dimension (IEF) under non-reducing strong denaturing conditions. All protein complexes are disrupted which are not linked by SS-bonds. In the 2nd dimension the chains are separated according to their molecular weight.

The Figure 3-5 shows that the 2D-pattern is different from the 1D-gel pattern. The antibody drug conjugate is disrupted into its single fragments. The disulfide bonds are split off due to the reduction process needed for the conjugation process. This is clearly seen in comparison with the naked mAb. The identification of individual fragments was done over the molecular weights, the isoelectric points, immunoblotting experiments and N-terminally sequence analysis after Westernblotting. Figure 3-6 shows the reaction of single fragments with the anti-toxophore antibody AB-1E8; TPP-1597 in comparison with the mAb. All bands of the ADC react. The mAb bands do not react with the anti-toxophore antibody, however the mAb bands react with an anti-human IgG1 antibody as expected.

Figure 3-5. 2D-gel Electrophoresis of BAY 1129980 (ADC) and BXR5P2D (mAb) Stained First by Coomassie Blue Brilliant G-250 and Second by Silver Stain. The gel was run under non-reducing conditions.

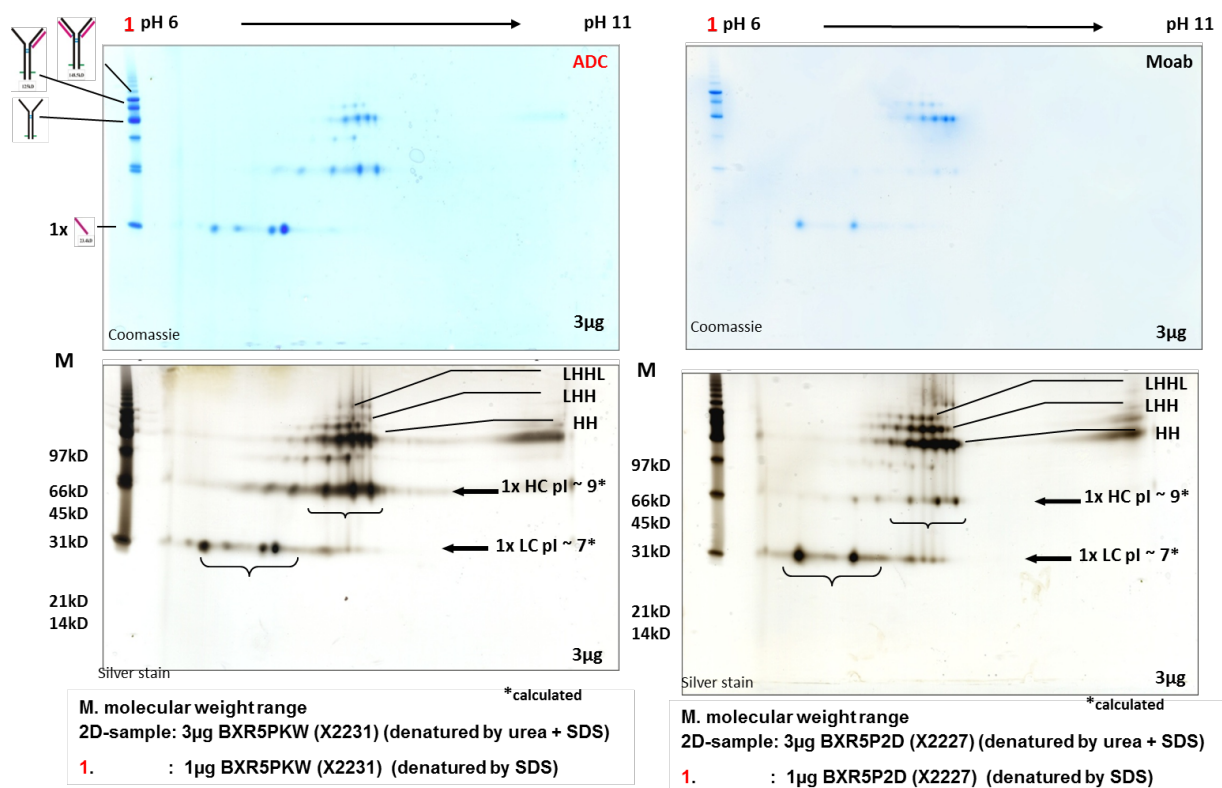
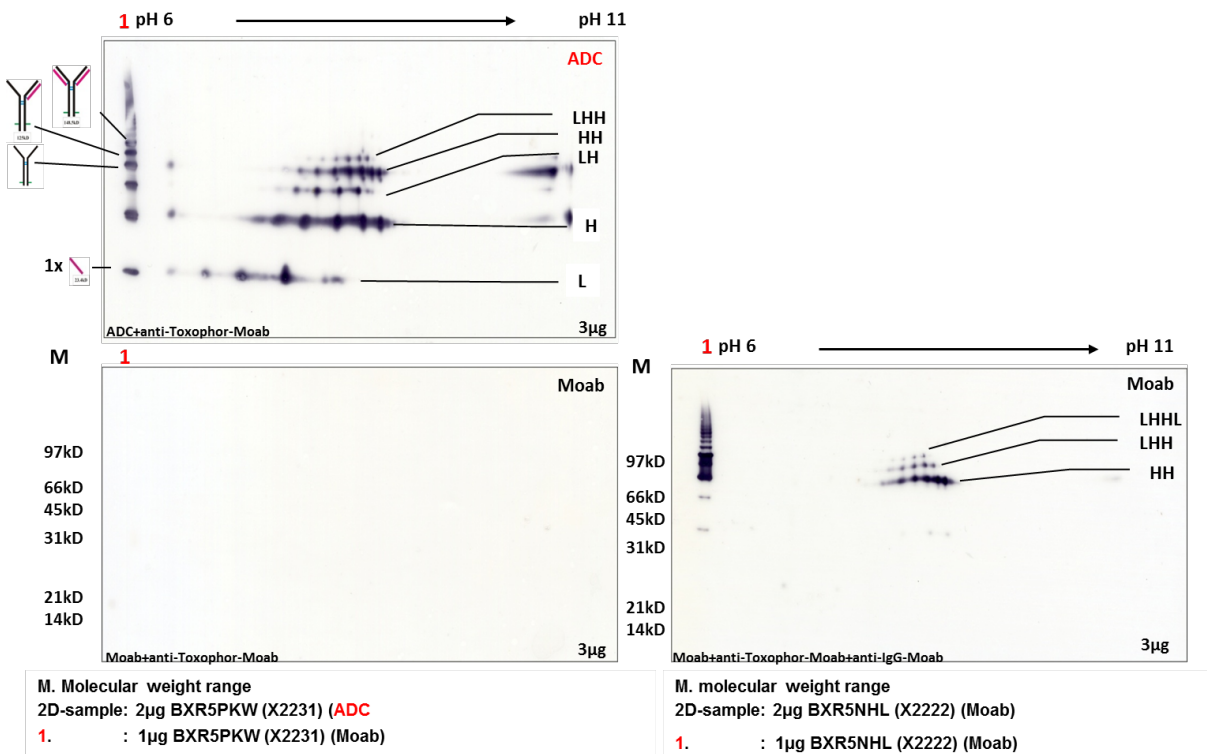


Figure 3-6. 2D-gel Electrophoresis of BAY 1129980 (ADC) and X2222 (mAb) were Blotted onto a PVDF-Membrane and Developed by an Anti-toxophore Antibody. The blot of the mAb was additionally reacted with an anti-human IgG antibody. The gels were run under non-reducing conditions.



3.4 Immunoblotting

BAY 1129980 was analyzed after gel electrophoresis using an anti-toxophore antibody to see the distribution of bound toxophore residues to the fragments in the 1D-gel. [Figure 3-7](#) shows the reaction with the anti-toxophore antibody under non-reducing and reducing conditions. There is a reaction with all fragments of the ADC indicating bound toxophores. The non-conjugated C4.4a antibody does not react as expected. [Figure 3-7](#) also gives the same blot that was additionally stained by Coomassie Blue Brilliant R-250.

BAY 1129980 GLP was also analyzed using a polyclonal antibody directed against the lambda light chain subtype. [Figure 3-8](#) shows the reaction with the polyclonal chicken anti-human lambda light chain antibody under reducing conditions. Only the light chain reacts as expected. Light and heavy chains are clearly visible after Coomassie blue staining ([Figure 3-8](#)). The conjugation process does not influence the binding of the anti-lambda light chain mAb to the lambda light chain..

Figure 3-7. Gel electrophoresis of BAY 1129980(ADC) and BXR5P2D (mAb) were run under reducing and non-reducing conditions on the same 4-12% SDS-gel and were then blotted onto a PVDF-membrane. The proteins were incubated with an anti-toxophore antibody. Afterwards, the blot was stained by Coomassie Blue Brilliant R-250.

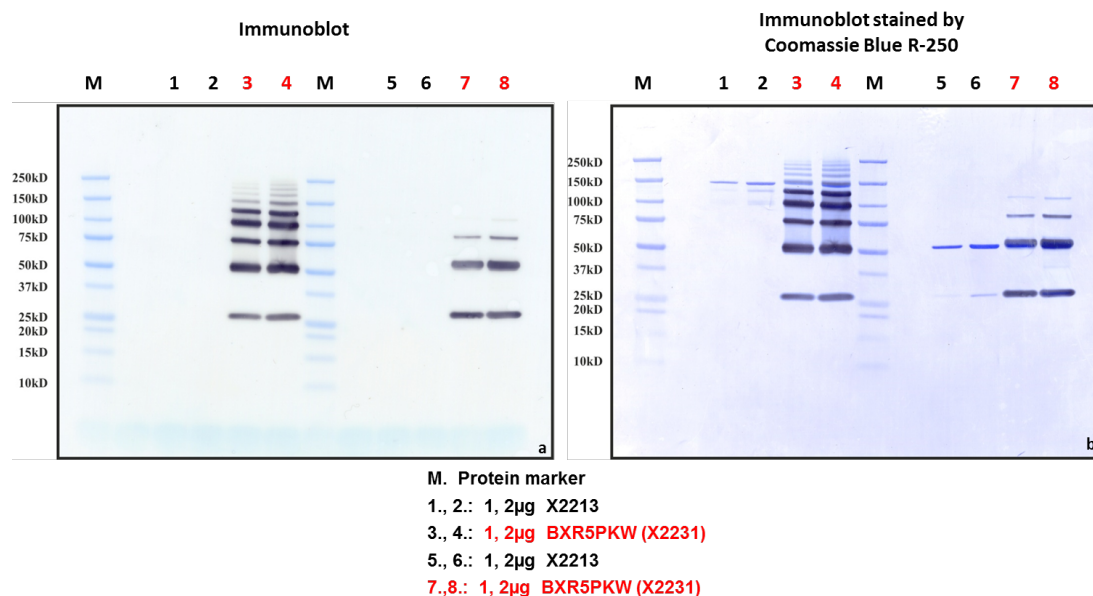
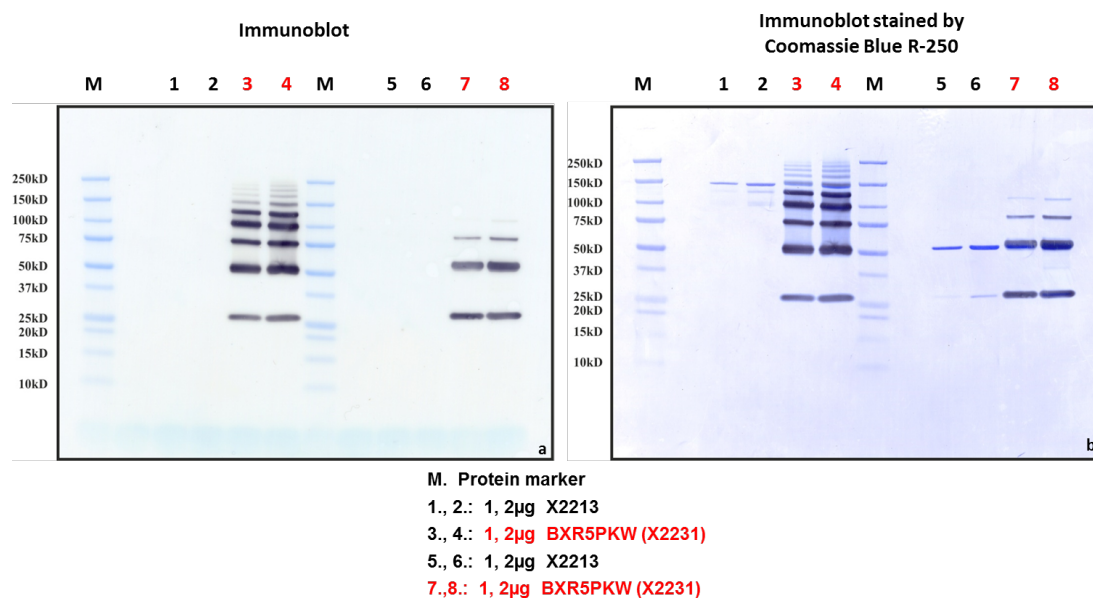


Figure 3-8. Gel electrophoresis of BAY 1129980(ADC) and BXR5P2D (mAb) were run under reducing and non-reducing conditions on the same 4-12% SDS-gel and were then blotted onto a PVDF-membrane. The proteins were incubated with an anti-toxophore antibody. Afterwards, the blot was stained by Coomassie Blue Brilliant R-250.



3.5 Reversed Phase HPLC Chromatography and UV-Spectrum

BAY 1129980 was analyzed using a stable bond HPLC-column at high temperature with a strong eluting solvent B in comparison with the naked antibody. [Figure 3-9](#) shows HPLC-profiles and overlays of the HPLC-profiles of BAY 1129980 and BAY 1112623 GLP-batches on a C18- and [Figure 3-10](#) on a C4-HPLC-column. BAY 1129980 splits into several peaks as a partially reduced and conjugated mAb under these conditions (high temperature, pH < 2). The non-conjugated mAb elutes as one peak at about 42min. The conjugate still seems to contain small amounts of the non-conjugated mAb. This is in agreement with the data from other studies. [Table 3-2](#) gives the retention times and area percent of main peaks from the C18- and C4-column and [Table 3-3](#) from the CN-column.

Table 3-2. Retention times and area % of main peaks run on a Zorbax SB C18 – and an X-Bridge C4-column. The peaks are marked in HPLC-profile (Figure 3-9, Figure 3-10). The non-conjugate mAb was run for comparison.

Batch (C18)	Peak 1 Rt. 37.7	Peak 2 Rt. 38.9	Peak 3 Rt. 41.7	Peak 4 Rt. 41.9	Peak 5 Rt. 42.4	Peak 6 Rt. 42.9	Rest
Batch (C4)	Peak 1 Rt. 2.5	Peak 2 Rt. 3.5	Peak 3 Rt. 8.9	Peak 4 Rt. 9.5	Peak 5 Rt. 10.9	Peak 6 Rt. 11.6	Rest
BXR5PKW (BAY 1129980)	2.3	18.8	19.9	20.3	20.1	13.5	5.1
BAY 1112623 (mAb)			97.2 Rt. 41.4				
BXR5PKW (BAY 1129980)	2.0	17.8	11.5	19.5	21.1	13.6	14.5
BAY 1112623 (mAb)			82.5 Rt. 8.4				

Figure 3-9. HPLC-profile of BXR5PKW (BAY 1129980 solution) on a C18-HPLC-column at 210 nm and Overlay of HPLC-profiles from BAY 1129980 and BAY 1112623 (mAb) on a C18-column. The samples were run as described under materials and methods.

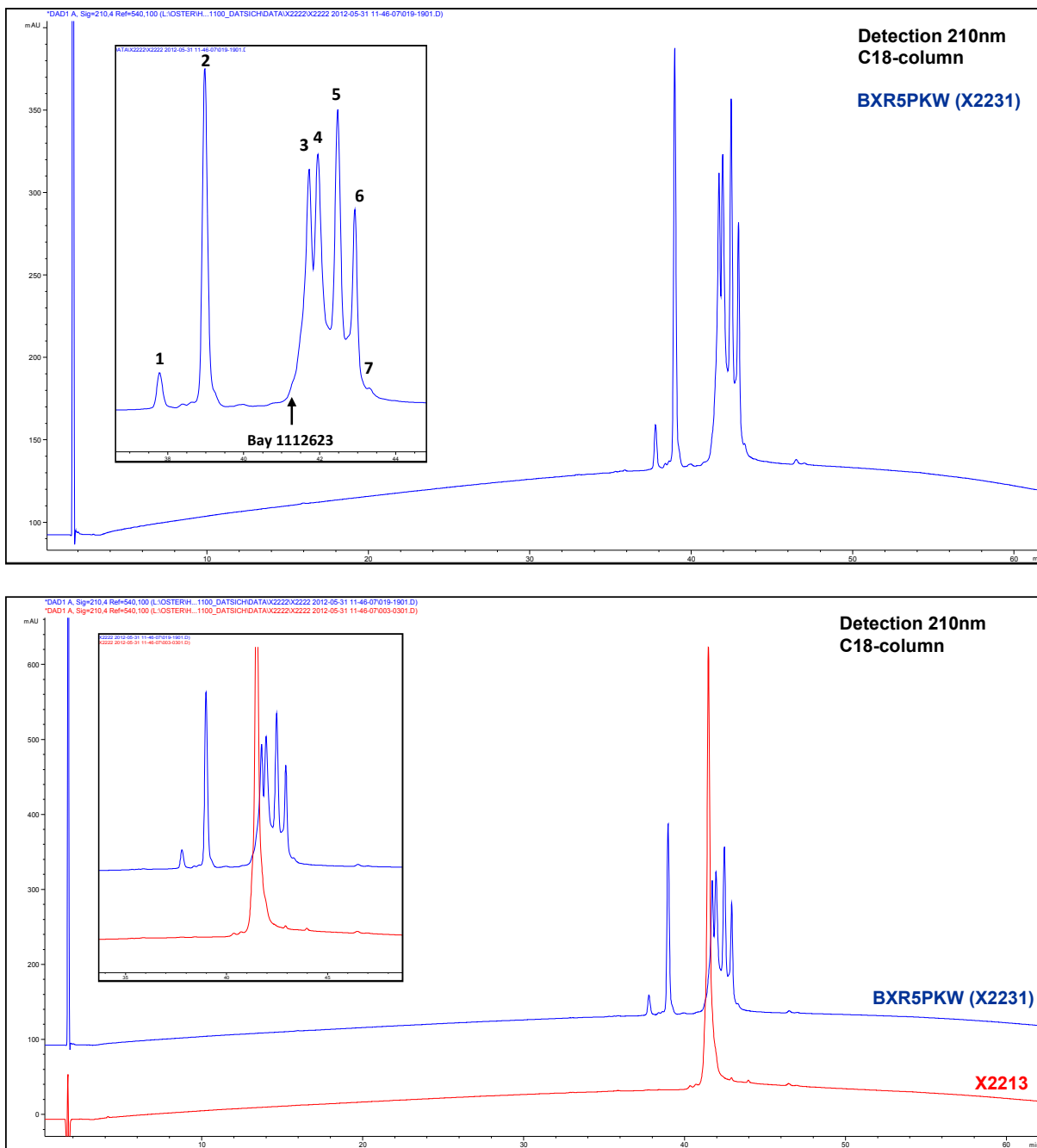


Figure 3-10 HPLC-profile of BXR5PKW (BAY 1129980, solution) on a C4-HPLC-column at 210 nm and Overlay of HPLC-profiles from BAY 1129980 and BAY 1112623 (mAb) on a C4-column. The samples were run as described under materials and methods.

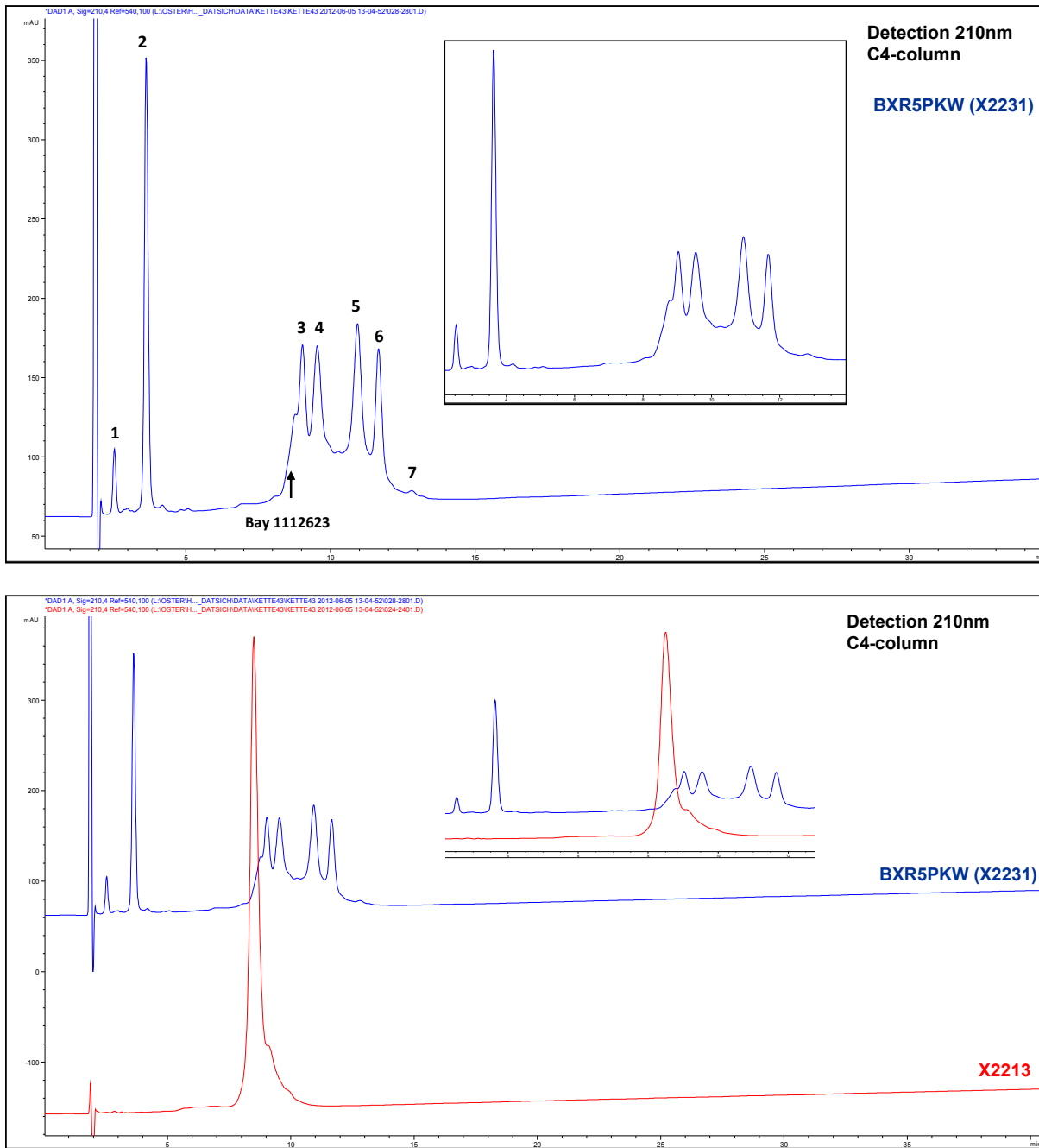


Table 3-3 gives the retention times and area percent of main peaks from the CN-column. The HPLC-profiles are presented in Figure 3-11. Again, the ADC elutes in several peaks from the column. The position of the free mAb is marked.

Table 3-3. Retention Times and Area % of main peaks of BAY 1129980 Run on a Zorbax SB CN-column. The peaks are marked in HPLC-profile (Figure 3-11). The non-conjugate mAb was run for comparison.

Batch (C18)	Peak 1 Rt. 19.8	Peak 2 Rt. 20.5	Peak 3 Rt. 22.0	Peak 4 Rt. 22.2	Peak 5 Rt. 22.7	Peak 6 Rt. 23.0	Rest
BXR5PKW (BAY 1129980)	2.1	18.4	2.2	34.0	22.2	16.6	4.5
BAY 1112623 (mAb)			98.6 Rt. 21.9				

Figure 3-12 and Figure 3-13 show the UV-spectra of the ADC and the mAb in the range from 190 up to 350 nm. Both compounds show very similar spectra as expected for proteins.

Figure 3-13b shows the whole spectrum collected by a DAD. The main chromophors are the peptide bonds (205 nm), cystine residues/phenylalanine (~250 nm) and tyrosine/tryptophan (~280 nm). The local maxima are given. The difference in the tryptophan content (about four Trp by DAR=4) between ADC and mAb cannot be seen clearly in the spectra.

Figure 3-11 HPLC-profile of BXR5PKW (BAY 1129980, ADC) on a CN-HPLC-column at 210 nm and Overlay of HPLC-profiles from BAY 1129980 and BAY 1112623 (mAb) on a CN-column.

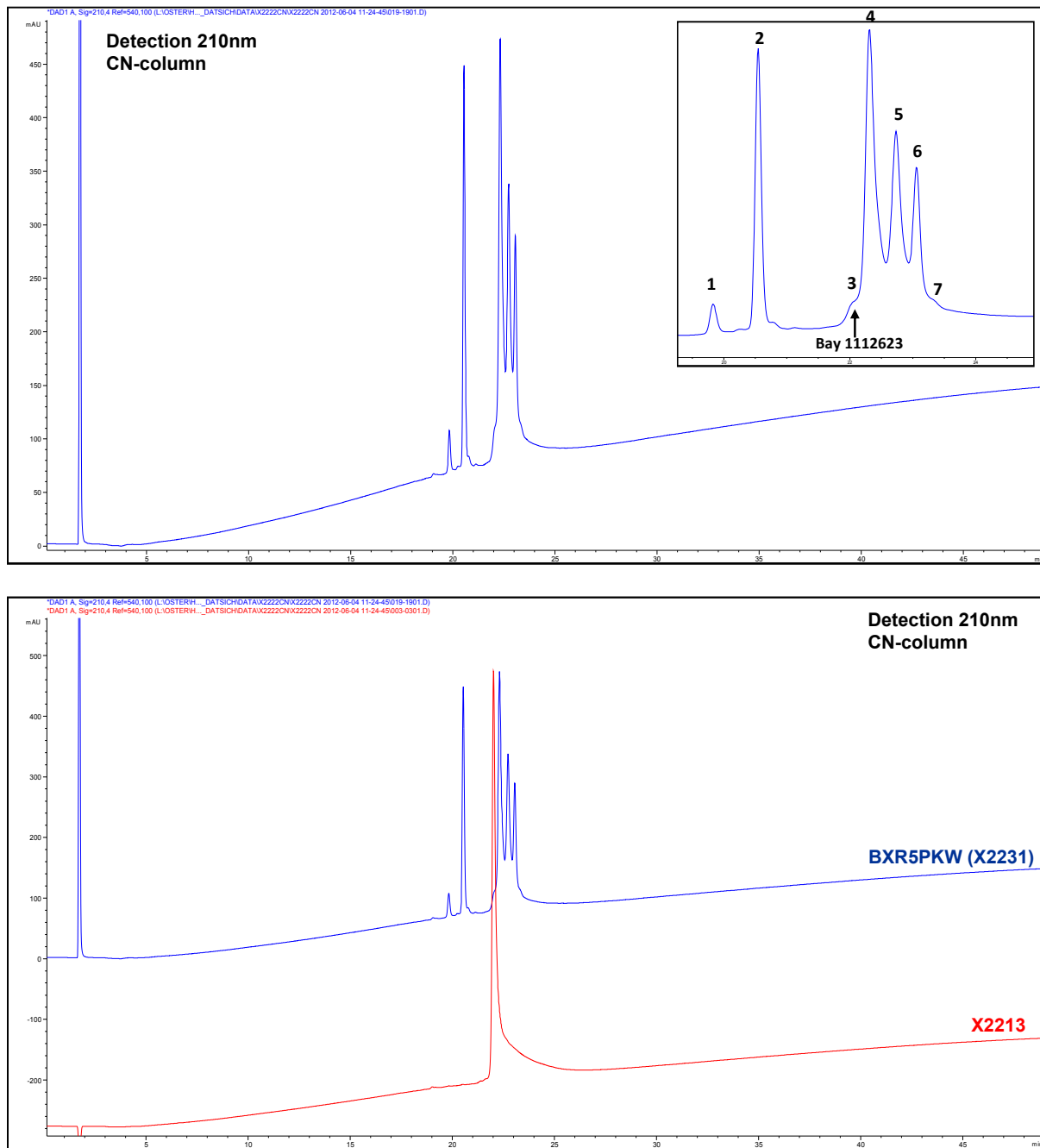
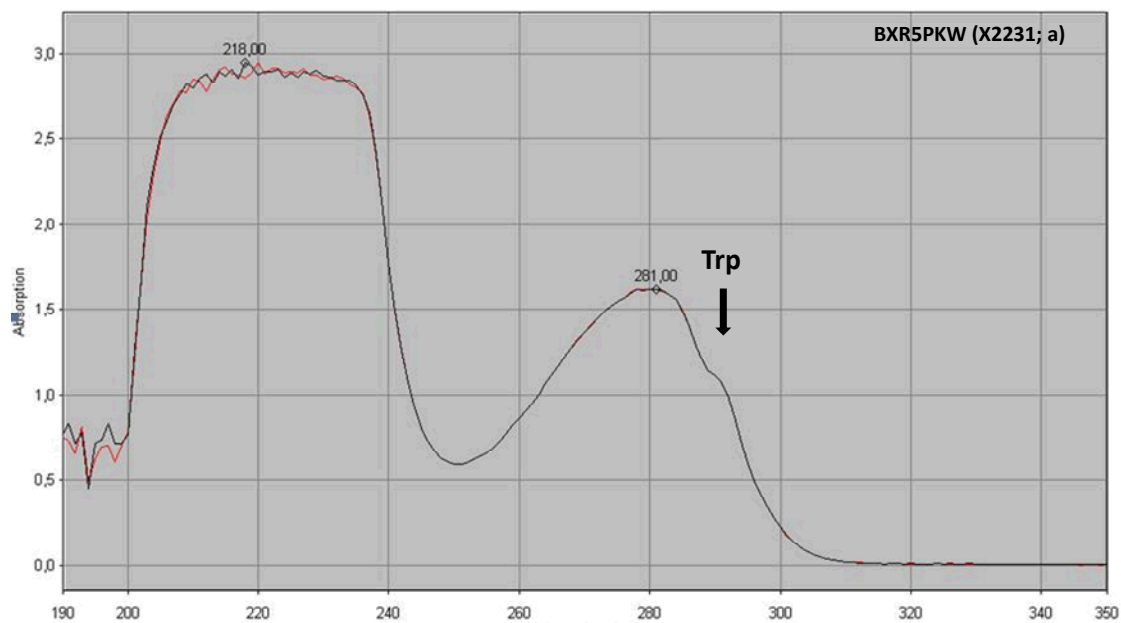


Figure 3-12 UV-spectra of BAY 1129980 and BXR5P2D in the range from 190-350 nm. The region from 250-300 nm is enlarged. The Trp-band at about 290 nm is clearly seen. The spectra were collected by a UV-spectrophotometer.

a.



b.

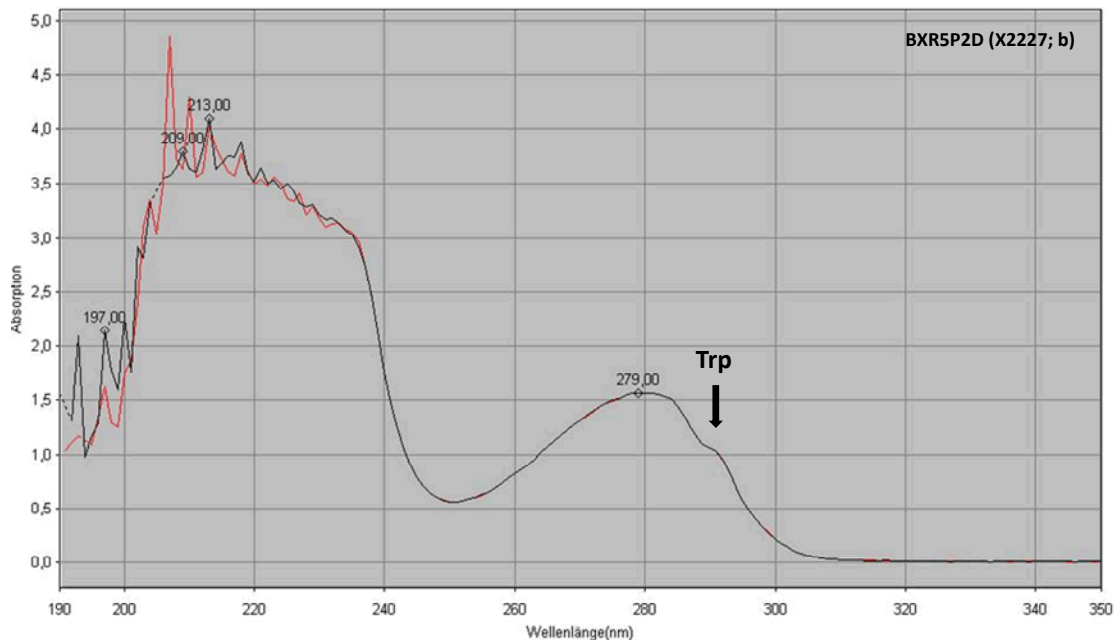
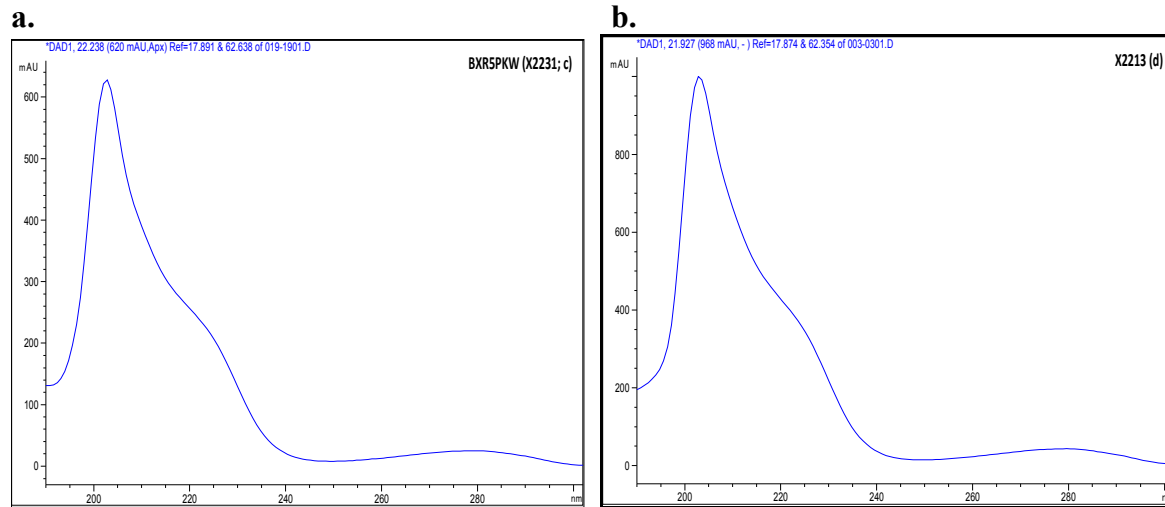


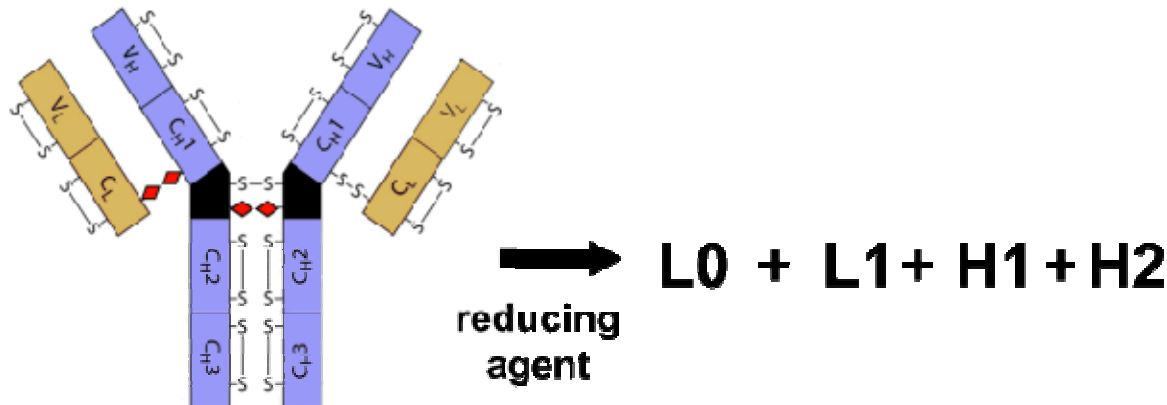
Figure 3-13. UV-spectra of BAY 1129980 and BXRP2D in the Range from 190-300 nm. The spectra were collected by a DAD during reversed phase chromatography (CN-column).



3.6 Separation of Light and Heavy Chains

The partially reduced BAY 1129980 antibody drug-conjugate was completely reduced by dithiothreitol in the strong denaturing agent 6M guanidinium chloride. Afterwards, the individual conjugated chains were separated by reversed phase high pressure liquid chromatography. The result should be single chains carrying different numbers of drug-linker residues. Figure 3-14 shows as an example the reduction of E4-2 derivate. The ratio of heavy to light chains should be a measure for the chain ratio because it only depends on the number of amino acids at 210 nm. It should be constant for the ADC and in the same order as for the naked mAb antibody.

Figure 3-14. Reduction of BAY 1129980 E4-2 under Strong Denaturing Conditions. The ADC splits off in single conjugated species.



BAY 1129980 was analyzed by HPLC for their conjugated light and heavy chains after reduction. The ratio of heavy/light chain was formed from the different conjugated peak areas at 210 nm. [Figure 3-15](#), [Figure 3-16](#) and [Figure 3-17](#) show HPLC profiles from the ADC and the non-conjugated mAb. The reduction was complete as shown by the overlay with the native antibody and the native ADC. [Table 3-4](#) gives the ratios of heavy/light chain and the retention times determined at 210nm. The ratio of heavy/light chain of BAY 1129980 is about 1.8. This is about 2:1 which is near to the theoretical value calculated from the amino acid number and near to the ratio of the non-conjugated mAb which is about 2.

$$\text{HC } 450\text{AA/LC } 217\text{AA} = 2.07$$

Table 3-4. Light and Heavy Chain Ratio and Retention Times of the BAY 1129980 and the mAb BAY 1112623 Determined from Peak Areas at 210 nm

Batch	Ratio Heavy/Light	Retention Time (min) Light Chain (main peaks)	Retention Time (min) Heavy Chain (main peaks)
BAY 1112623 (mAb)	2.00	3.97	11.82
BXR5PKW (BAY 1129980, ADC)	1.81	3.28, 4.01, 5.44	11.97, 13.23, 14.53, 15.77

Figure 3-15. HPLC-profile of BAY 1129980 under reducing conditions; conjugated forms of light and heavy chain are marked. The peaks used for ratio formation are given. The ADC was separated on a RP-4-column. A schematic picture of reduction is given.

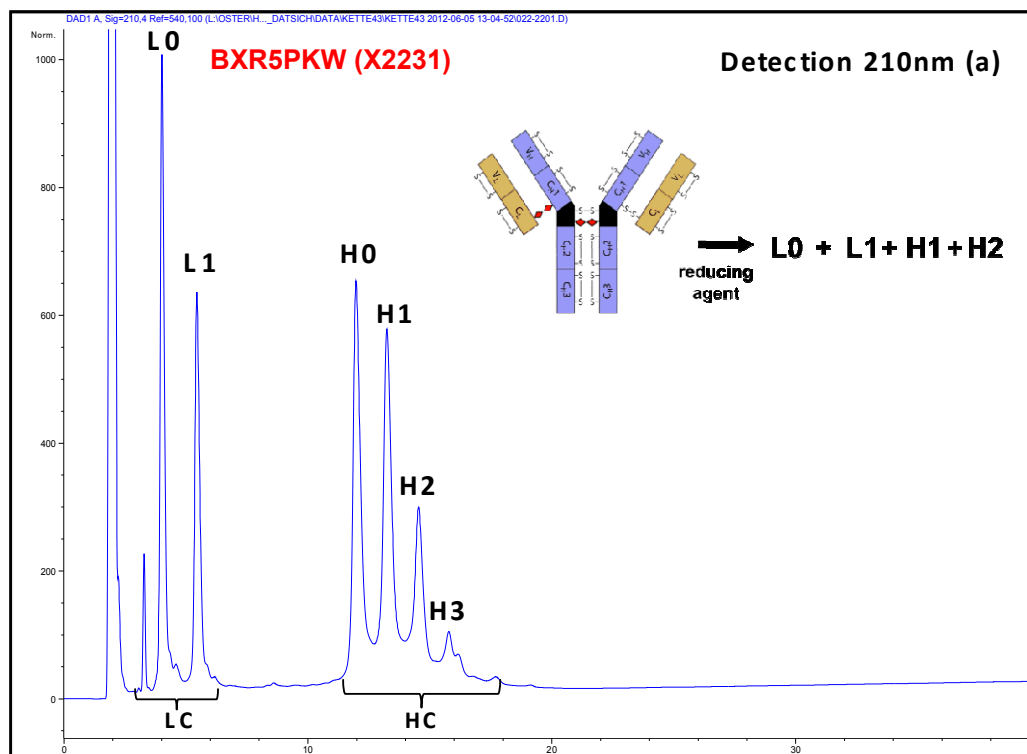


Figure 3-16 Overlay of HPLC-profiles of BAY 1129980 (ADC) and BAY 1112623 (mAb) under reducing conditions; non-conjugated forms of light and heavy chain are marked. The position of the native mAb is shown.

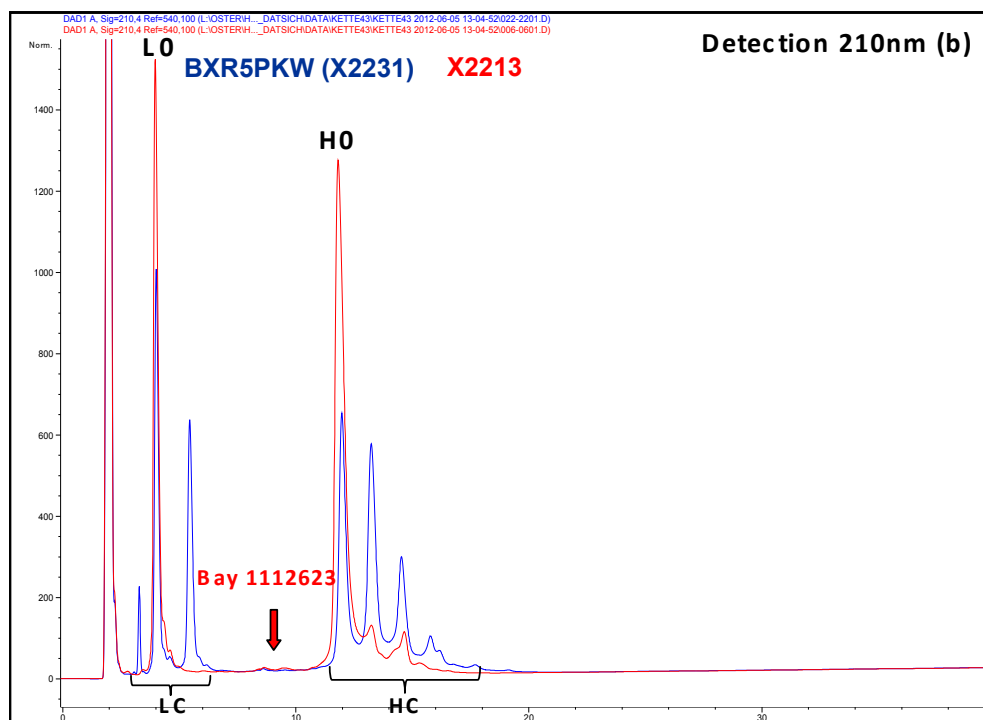
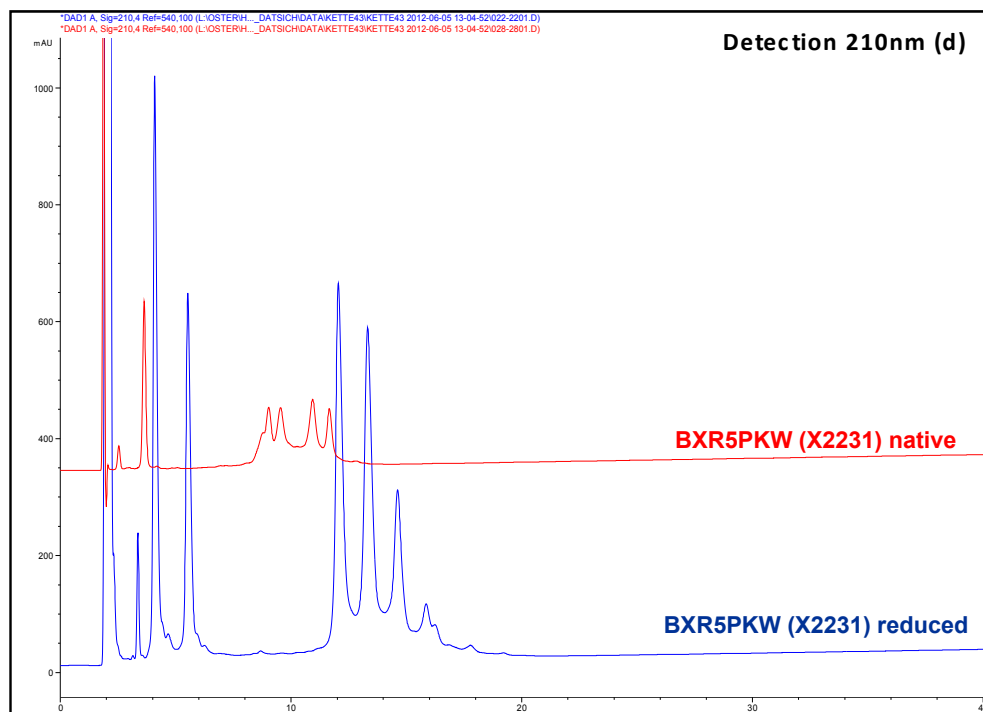


Figure 3-17 Overlay of HPLC-profiles of native BAY 1129980 (ADC) and under reducing conditions.



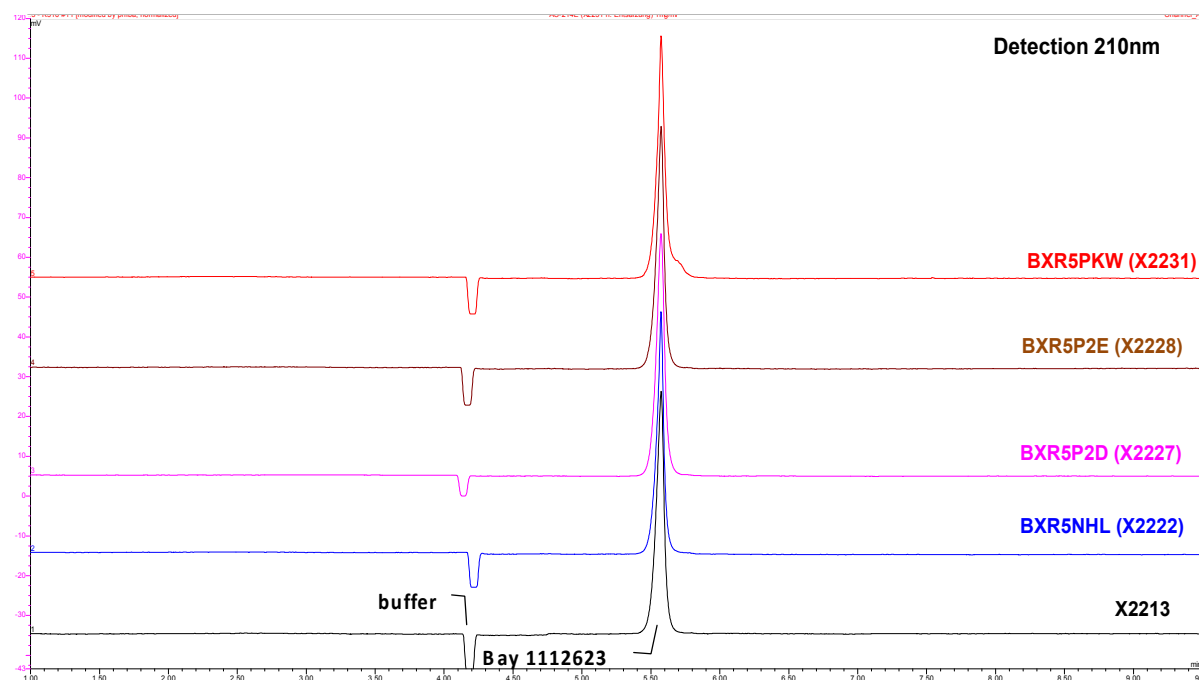
3.7 Capillary Zone Electrophoresis

Capillary electrophoresis of BAY 1129980 and BAY 1112623 GLP-batches were performed using a buffer of high pH to elute the protein. [Figure 3-18](#) shows an overlay of the elution profiles of the sample and [Table 3-5](#) gives the retention times of the ADC and mAb peaks. The ADC and the mAb elute as one main peak at about 5.5 min.

Table 3-5. Retention of Main Peak of the BAY 1112623 GLP-batches Run on a C18- and a CN-column

Batch	Retention Time (min) Antibody Peak
BAY 1112623	5.54
BXR5NHL	5.41
BXR5P2D	5.56
BXR5P2E	5.51
BXR5PKW (BAY 1129980)	5.42

Figure 3-18. CZE-profiles of BAY 1129980 and BAY 1112623 GLP-Batches on a Fused Silica Glass Capillary Column run using a high pH CAPS-buffer



3.8 Size Exclusion Chromatography

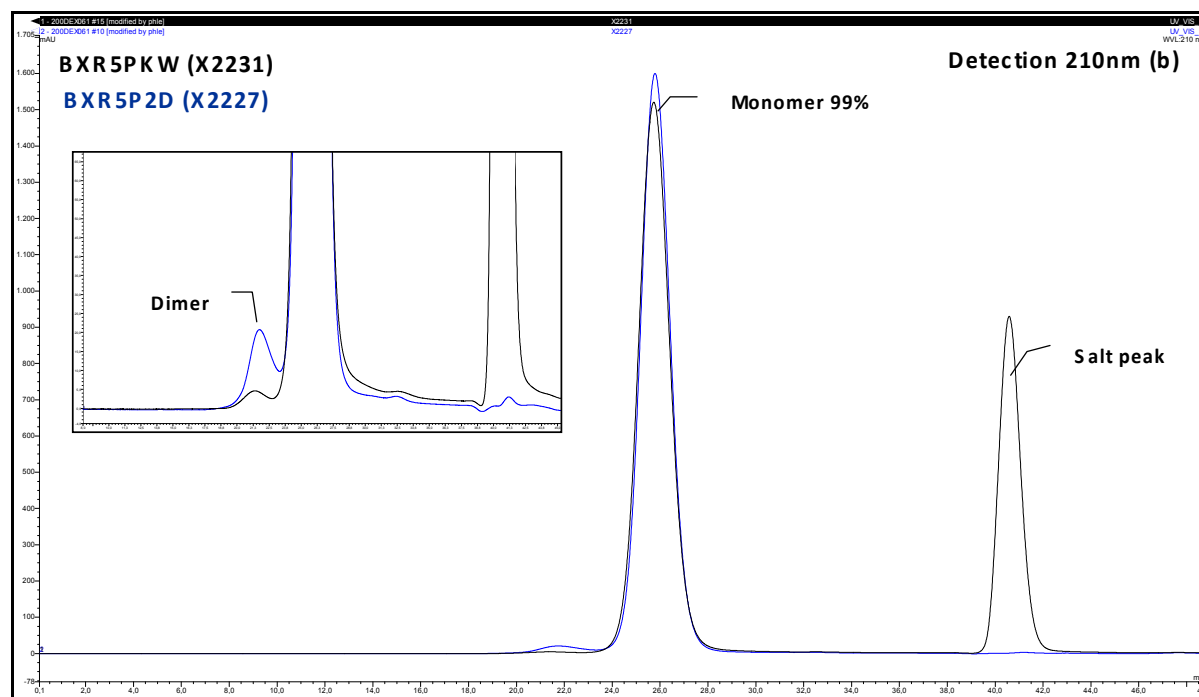
BAY 1129980 was analyzed in comparison with BAY 1112623 GLP-batch BXR5P2D on a Superdex-200 column at 210 nm. [Figure 3-19](#) shows the size exclusion profile of BAY 1129980 and an overlay with the non-conjugated mAb. The conjugate shows less dimer than the non-conjugated mAb. [Table 3-6](#) gives the monomer, dimer and oligomer content and the corresponding retention times. The dimer + oligomer content of BAY 1129980 is below 1%. The apparent molecular weight of the conjugated mAb is with

about 110 kD in the same order of magnitude than that of the naked mAb. This is lower than the known one for an IgG1 mAb of 150 kD indicating a very compact structure in comparison to the globular proteins used for the molecular weight calibration curve. Non-bound lambda light chain is only present in small amounts (< 1%).

Table 3-6. Size-exclusion chromatography of BAY 1129980 (ADC) and BXRP2D (mAb), retention time of the main peak, monomer, dimer and oligomer content determined from peak areas and molecular weights of monomer are given. Salt peaks were not integrated.

Batch	Monomer % Area	Dimer+Oligomer % Area	Free LC % Area	Monomer (Rt. min)	MW monomer (kD)
BXR5P2D	98.04	1.82	0.15	25.79	109
BXR5PKW (BAY 1129980)	99.39	0.37	0.25	25.74	110

Figure 3-19. Overlay of the SEC profile (total and cut off) of BAY 1129980 on a Superdex 200 with the mAb batch BXR5P2D on the same column in PBS-buffer pH 7.3; detection 210 nm.



3.9 Ion-Exchange Chromatography

BAY 1129980 was analyzed on a cation-exchange column in comparison with the non-conjugated antibody. Figure 3-20 shows the IEC-profile of BAY 1129980. The ADC is separated into several peaks. The naked mAb is clearly separated from the conjugated species (see Figure 3-21). It is identified by overlaying with the naked mAb and by spiking. Table 3-7 gives the area percent of the ADC: free mAb (peak 1+2), peak 3, peak 4 and additional peaks.

The mAb itself shows little charge heterogeneity because of removing C-terminal lysine from the heavy chain and converting the N-terminal glutamines in glutamic acid in the DNA sequence.

Ion-exchange chromatography is also a sensitive method for stability assessment of the ADC. [Figure 3-22](#) gives a diagram of selected peaks from stability samples stored at -70°C, 2-8°C, 25°C and 40°C for one month. There is an increase in free mAb and a decrease of peak 3 and 4 over time. This already begins at 25°C after one week ([Figure 3-23](#)).

Table 3-7. Ion-exchange chromatography of BAY 1129980; non-conjugated mAb, peak 1, peak 2 and additional peaks determined from peak areas are given.

Batch	Non-conjugated mAb (Peak 1+2, Rt. 24.91+26.54)	Peak 3 (Rt.31.25)	Peak 4 (Rt.36.15)	Sum Additional Peaks
BXR5PKW (BAY 1129980)	6.1	21.5	25.8	46.6

Figure 3-20. IEC-Profile of BAY 1129980 on a WCX-10 column in MES-buffer pH 6.3; detection 280 nm. The free mAb and the two main peaks are marked.

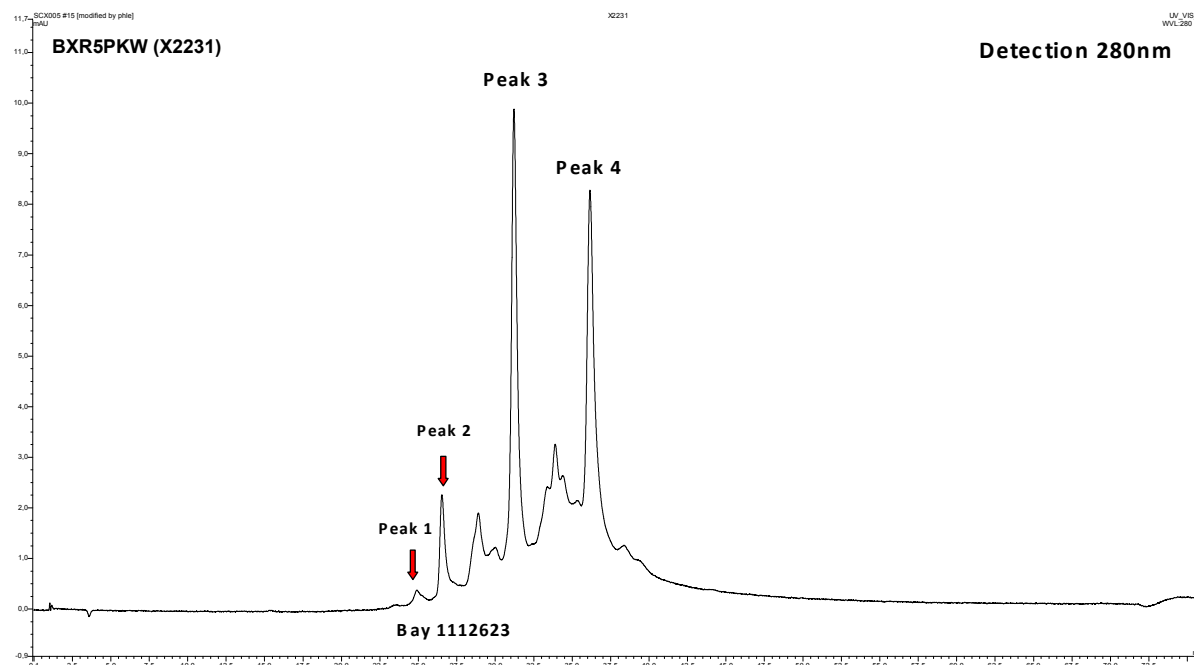


Figure 3-21. Overlay of IEC-profiles of BAY 1129980 and BAY 1112623 BXR5P2D on a WCX-10 column in MES-buffer pH 6.3; detection 280 nm. The free mAb and the ADC-region are marked.

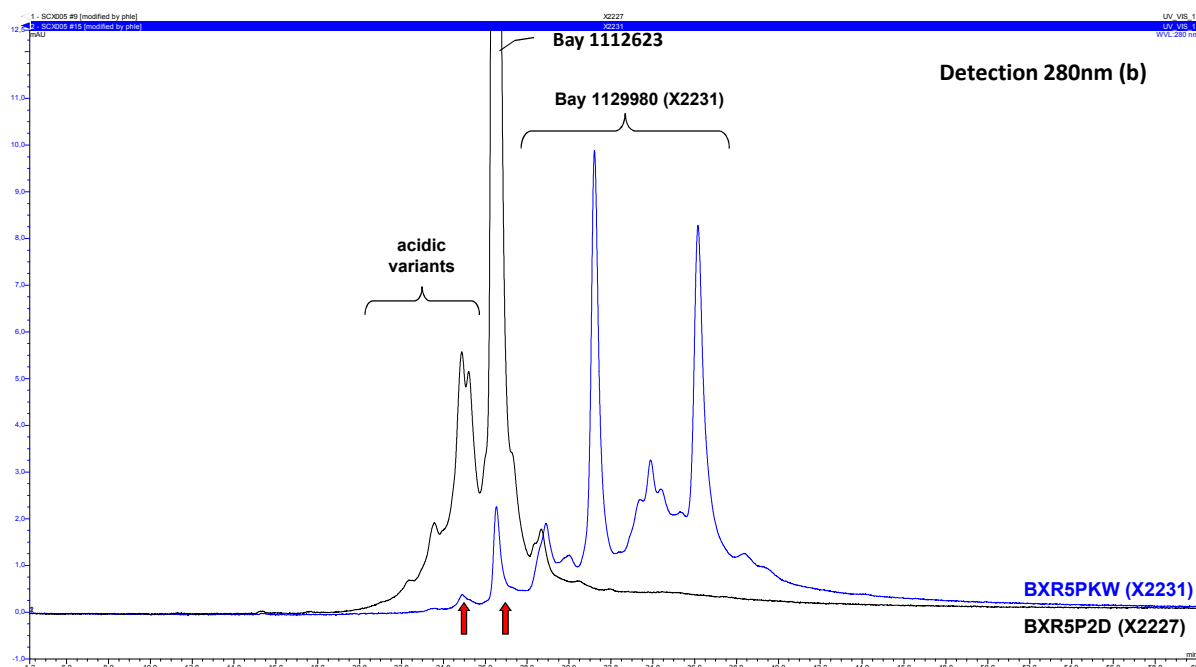


Figure 3-22. Diagram of stability samples from IEC-analyses of ADC-batch BXR5PKW (BAY 1129980) stored at different temperatures for one month; free mAb peaks 1 and 2, sum of free mAb, peak 3 and 4 as well as sum of other peaks are given as area %.

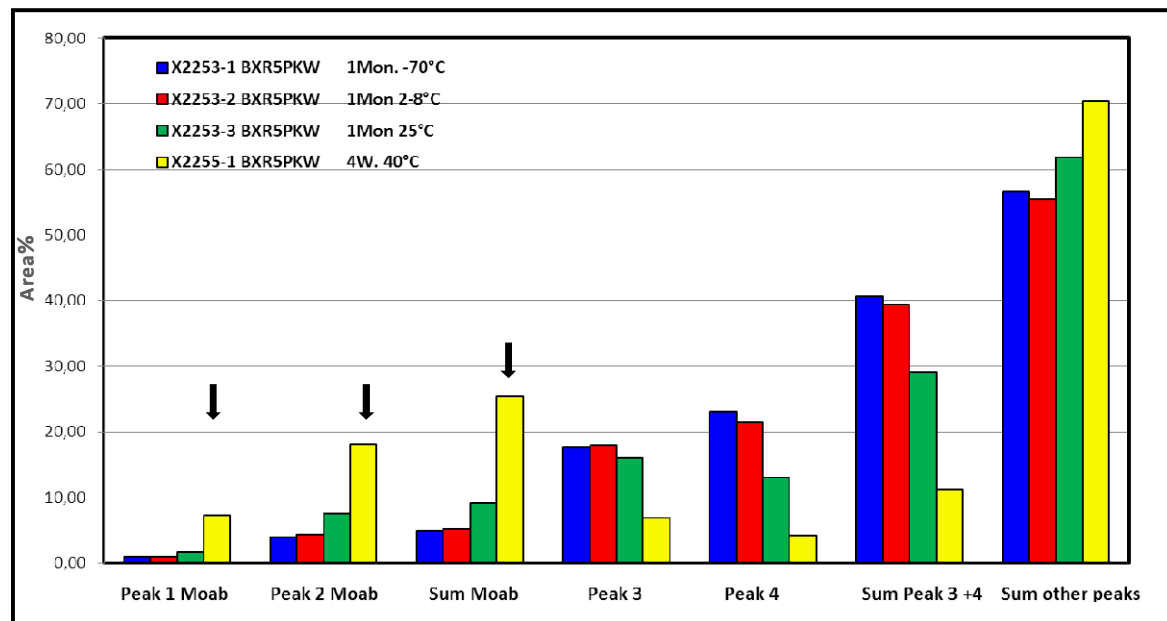
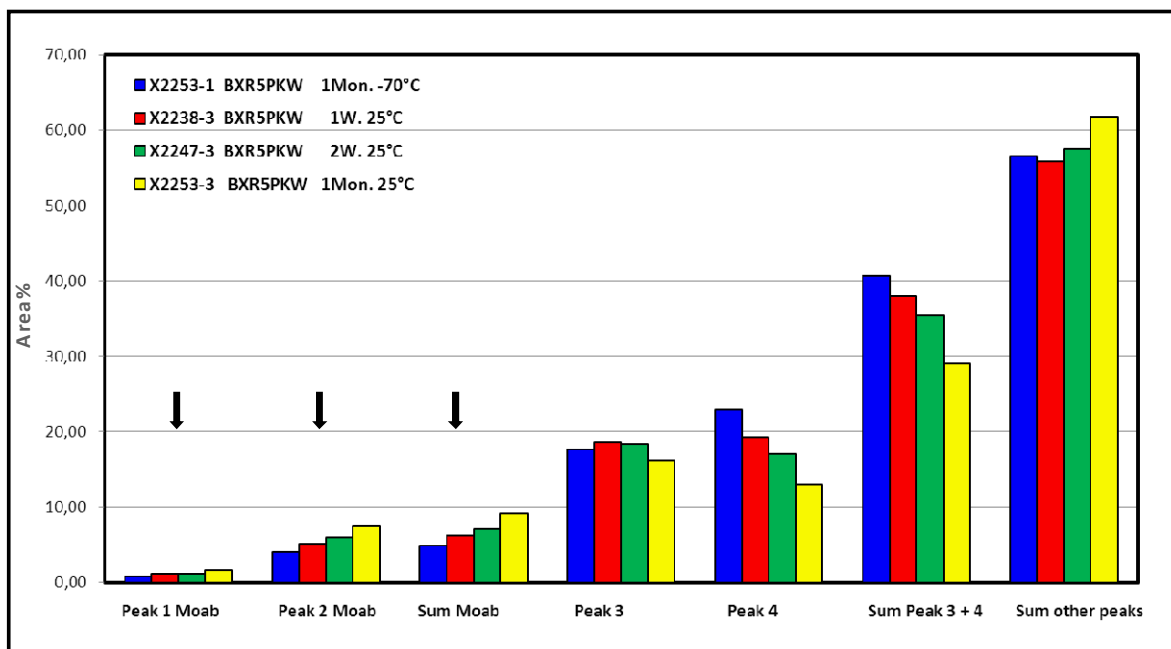


Figure 3-23. Diagram of stability samples from IEC-analyses of ADC-batch BXR5PKW (BAY 1129980) stored at -70°C for one month and 25°C for 1 and 2 weeks as well as 1 month; free mAb peaks 1 and 2, sum of free mAb, peak 3 and 4 as well as sum of other peaks are given as area %.



3.10 Molecular Weight Determination by HPLC-MS

Antibody drug conjugates are heterodimeric molecules with a molecular weight of about 150 kD. They are very complex molecules composed of two light and two heavy chains with some bound toxophore residues. In addition to the protein component ADC's contain an N-linked biantennary sugar in the conserved region on each heavy chain of the antibody. The molecular weight of BAY 1129980 was determined by HPLC electrospray ionization mass spectrometry (HPLC-ESI-MS) native and after reduction by DTT. [Table 3-8](#) shows the determined molecular weights. The determined molecular weights of the light chain species L0 and L1 are in good agreement with the calculated molecular weights of the reduced forms ([Figure 3-24](#)). No higher forms of light chain e.g., L2, L3 were found showing that only the inter-chain SS-bond was reduced and conjugated.

The determined molecular weights of the heavy chain species H0, H1, H2 and H3 reflect the posttranslational modifications by N-glycosylation. All three drug-loaded species were found which theoretically result from complete reduction of inter-chain SS-cross-links. The drug-to-antibody ratio (DAR) was calculated after reduction of the ADC to 4.1. This is in good agreement to the results from amino acid analysis, HPLC-analysis and to the expected value of 4. The main forms under native conditions are LH2, HH2 and LHH1 ([Figure 3-25](#)).

Table 3-8. Molecular weight determination of BAY 1129980 determined by HPLC-ESI-MS.

Batch	Average MW in Da calculated	Average MW in Da determined	Δ Mass	Comment
BXR5PKW (BAY 1129980) (native)	23940.8	23941.7	0.9	L1 (LC+1Toxin)
	49826.4	49829.8	3.4	H1 (HC+1Toxin)
	51953.2	51957.5	4.3	H3 (HC+3Toxins)
	73767.3	73771.4	4.2	LH2 (LC+HC+2Toxins)
	99652.9	99659.5	6.6	HH2 (HC Dimer+2Toxins)
	101779.7	101787.0	7.3	HH4 (HC Dimer+4Toxins)
	103906.5	103912.7	6.2	HH6 (HC Dimer+6Toxins)
	121466.9	121473.3	6.4	LHH1 (IgG -LC+1Toxin)
	123593.7	123605.4	11.7	LHH3 (IgG -LC+3Toxins)
	143280.9	143283.2	2.3	LHHL (IgG)
BXR5PKW (BAY 1129980) (reduced)	22882.5	22881.3	-1.2	L0 (reduced light chain)
	23945.9	23944.4	-1.5	L1 (LC +1Toxin)
	50219.5	50218.1	1.4	H0+GOF
	51282.9	51281.4	-1.5	H1+GOF (HC+1Toxin)
	52346.3	52345.1	-1.2	H2+GOF (HC+2Toxin)
	53409.7	53408.1	-1.6	H3+GOF (HC+3Toxin)

Figure 3-24. Profile of the deconvoluted ESI-MS-spectra of BAY 1129980 under reducing conditions. The different conjugated species are marked.

$L0_{\text{found}}$ Δ -1.2Da, $L1_{\text{found}}$ Δ -1.5Da
 $H0_{\text{found}}$ Δ -1.4Da, $H1_{\text{found}}$ Δ -1.5Da, $H2_{\text{found}}$ Δ -1.2Da, $H3_{\text{found}}$ Δ -1.6Da

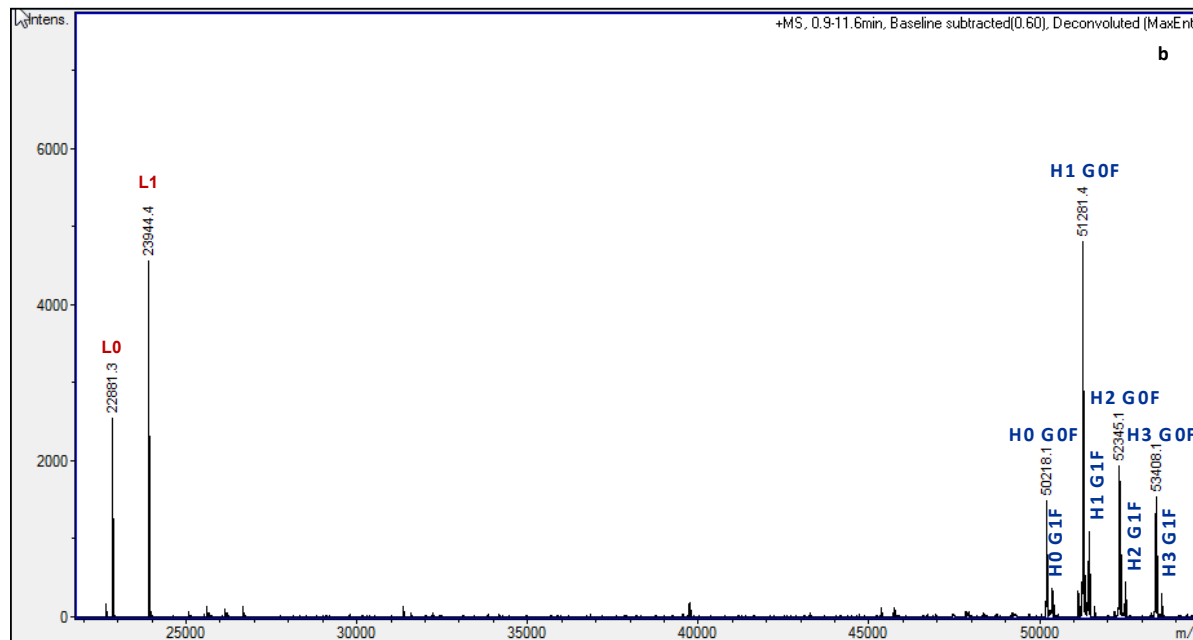
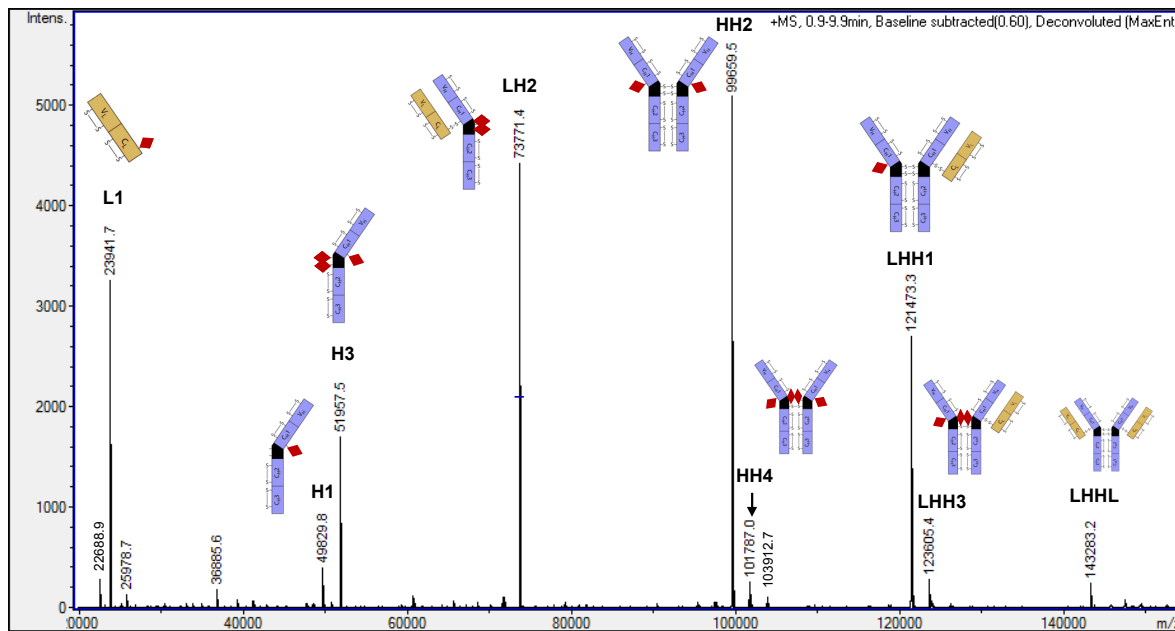


Figure 3-25. Profile of the deconvoluted ESI-MS-spectra of BAY 1129980 under native conditions. The molecular weight ranges of approx. 20 up to 150 Da are shown. Single conjugated species are marked.

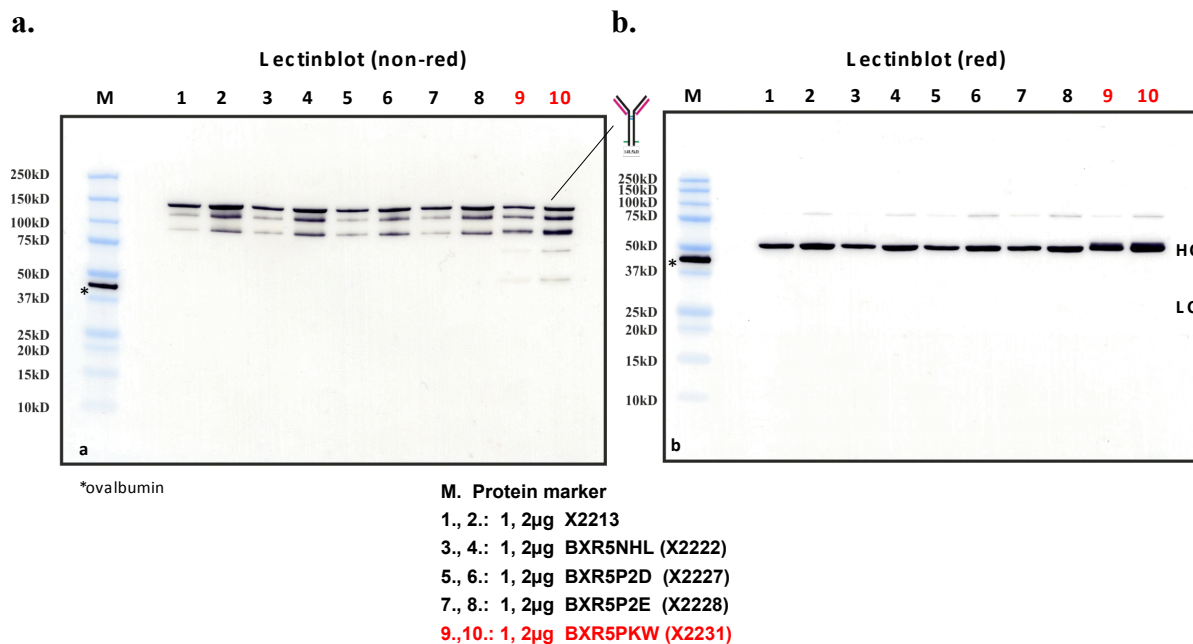


4. Methods Dealing with Protein Bound Carbohydrates

4.1 Lectinblotting

BAY 1129980 (ADC) and BAY 1112623 GLP-batches were compared using the technique of lectinblotting with the biotinylated lectin Concanavalin A (Con A), which is specific for mannose-type side chains. [Figure 4-1 \(a\)](#) shows the Con A lectinblot under non-reducing and [Figure 4-1 \(b\)](#) under reducing conditions. The staining profile shows that mannose type sugars are only bound to the heavy chain as expected due to the consensus sequence present at the heavy chain. The light chain shows no reaction with the lectin as expected. Both, the mAb and the conjugate show a reaction with the lectin. The conjugate shows a substructure coming from conjugated heavy chain species. The lectinblots show that the conjugation process has no influence on the glycan structure of the ADC.

Figure 4-1. Westernblots of a 4-12%- and a 12%-SDS-gel of BAY 1112623 GLP-batches under non-reducing (a) and reducing conditions (b). The gels were blotted onto PVDF membranes and then stained by Concanavalin A. Ovalbumin was used as positive control.



4.2 Sialic Acid Determination

BAY 1129980 and BAY 1112623 were compared for their sialic acid type and content. The analyses only show traces of N-acetyl neuraminic acids in BAY 1129980 (approx. 0.02 g/100 g mAb corresponds to about 0.1 mol NANA/mol BAY 1112623; [Table 4-1](#)). [Figure 4-2](#) shows overlays of the HPLC profiles of BAY 1129980 (ADC) and BXR5P2E (mAb) and of the control glycoprotein fibrinogen. The conjugation process has no influence on the sialic acids.

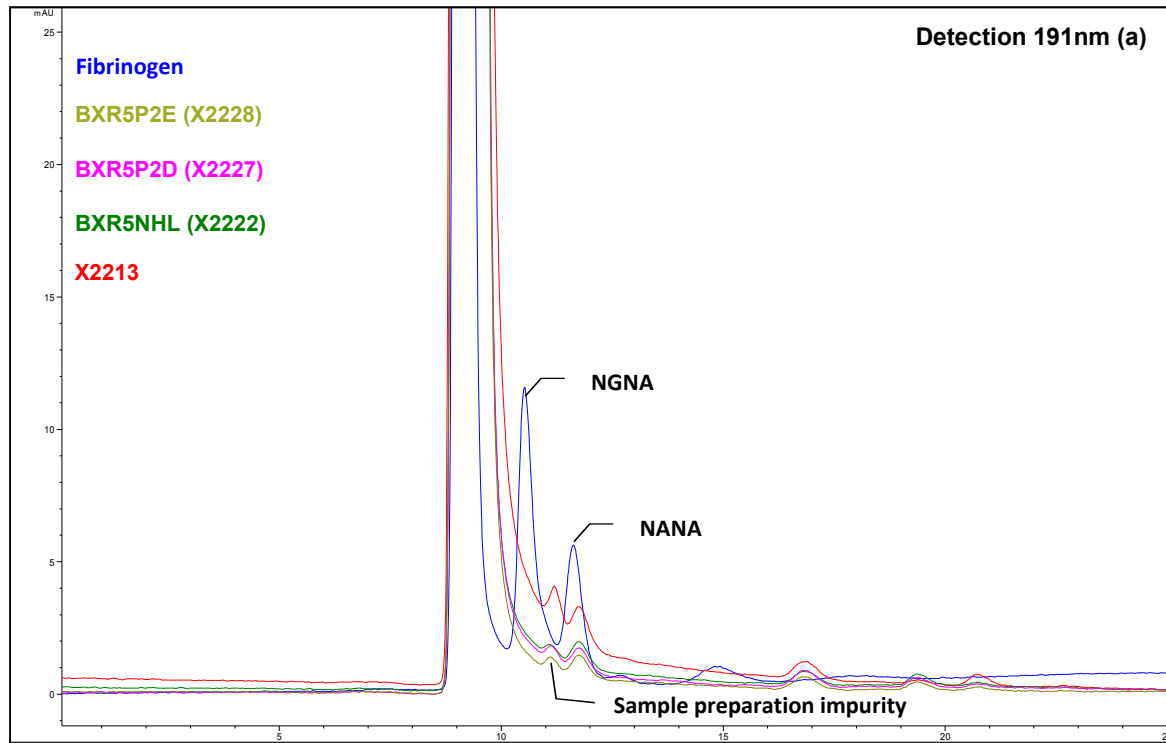
Table 4-1. N-acetyl neuraminic acid (NANA) and N-glycolyl neuraminic acid (NGNA) determination of BAY 1112623 GLP-batches given in gNANA/100g protein and gNGNA/100g protein.

Batch	g NANA/100 g Protein	g NGNA/100 g Protein
BAY 1112623	0.02	n.d. ^a
BXR5NHL	0.02	n.d. ^a
BXR5P2D	0.01	n.d. ^a
BXR5P2E	0.02	n.d. ^a

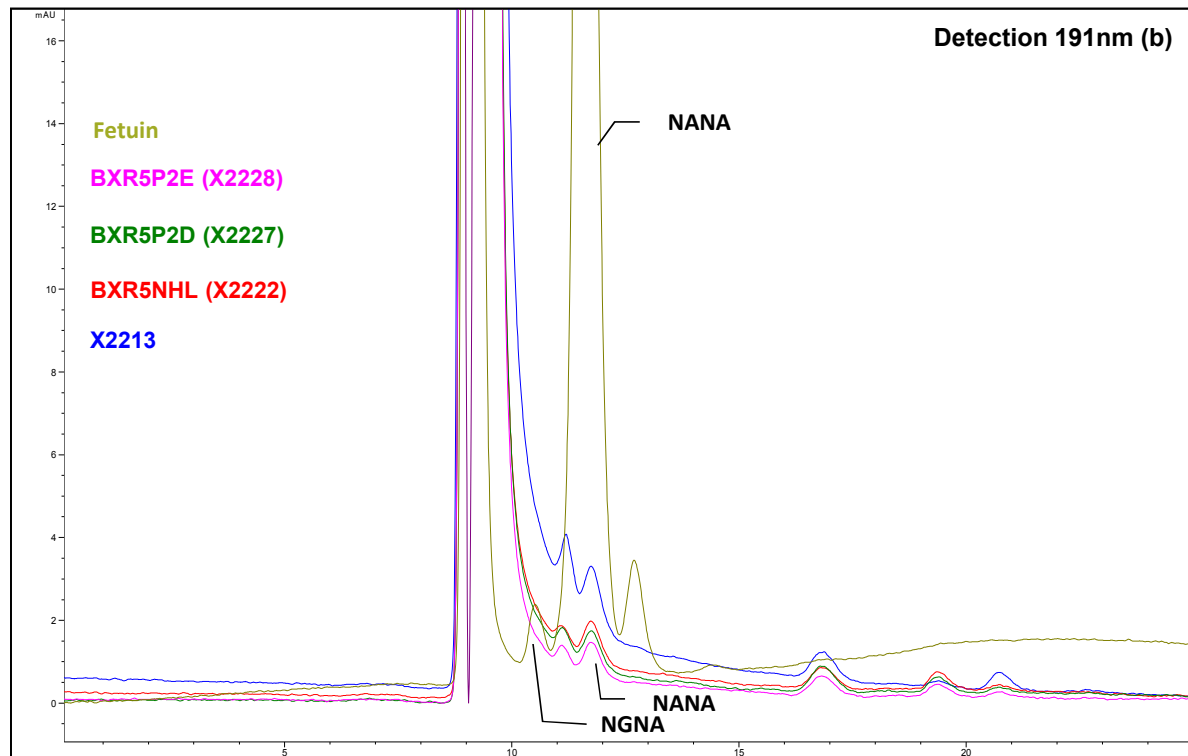
^a n.d. not detected

Figure 4-2. Overlay of HPLC-profiles of sialic acid determination of BAY 1129980 (ADC) and mAb in comparison with a NGNA + NANA reference (a) and with the glycoprotein Fibrinogen (b).

a.



b.



4.3 Monosaccharide Determination

BAY 1112623 (IgG1) contains N-linked bound glycans in the constant region of the heavy chain on a conserved asparagine at position Asn(302). The influence of conjugation on the sugar structures was analyzed by neutral sugar analysis of ADC- and mAb-batches.

BAY 1129980 (ADC) and BAY 1112623 GLP-batches were analyzed for their type and content of monosaccharides by high performance liquid anion exchange chromatography and pulsed aperiometric detection. Beside the neutral sugar derivatives the hexosamines could be separated and identified simultaneously. Hexosamine determination is useful for differentiation between N- and O-glycosylation. Minor amounts of hexoses present in glycans are destroyed by acid hydrolysis conditions as for example galactose. Mannose is also partially destroyed.

The total sugar content is practically identical before and after conjugation (see [Table 4-2](#)). There is no influence by conjugation. Fig. 4-3 shows overlays of the HPLC-profiles of BAY 1129980 (ADC) and BXR5P2D (mAb) and of a monosaccharide reference.

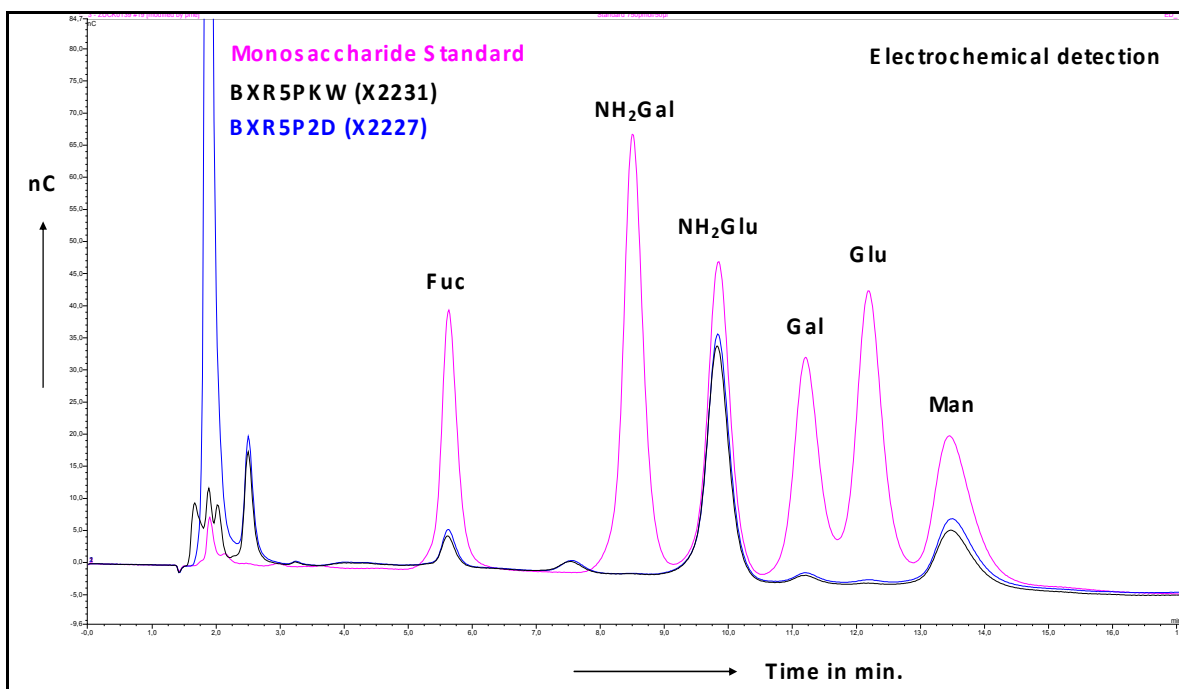
Table 4-2. Monosaccharide content of BAY 1112623 GLP-batches is given in g mono-saccharide/100 g protein. The values are not corrected for hydrolyses losses of the individual sugars.

Monosaccharide	BAY 1112623	BXR5NHL	BXR5P2D	BXR5P2E	BXR5PKW (BAY 1129980)
Fucose	0.15	0.15	0.14	0.15	0.12
Galactosamine	n.d. ^a	n.d. ^a	n.d. ^a	n.d. ^a	n.d.
Glucosamine	1.31	1.30	1.28	1.43	1.31
Galactose	0.06	0.04	0.04	0.05	0.04
Glucose^b	0.02	0.01	0.01	0.01	n.d.
Mannose	0.57	0.54	0.50	0.55	0.46
Sum	2.11	2.05	1.98	2.19	1.94

^a n.d. not detected

^b ubiquitous contamination in biological samples

Figure 4-3. Overlays of HPLC-profiles of monosaccharide determination of BXR5PKW (ADC), BAY 1112623 GLP-batch BXR5P2D and of a monosaccharide reference. The sugars were separated by anion-exchange chromatography and electrochemically detected.



4.4 Oligosaccharide Profile Analysis

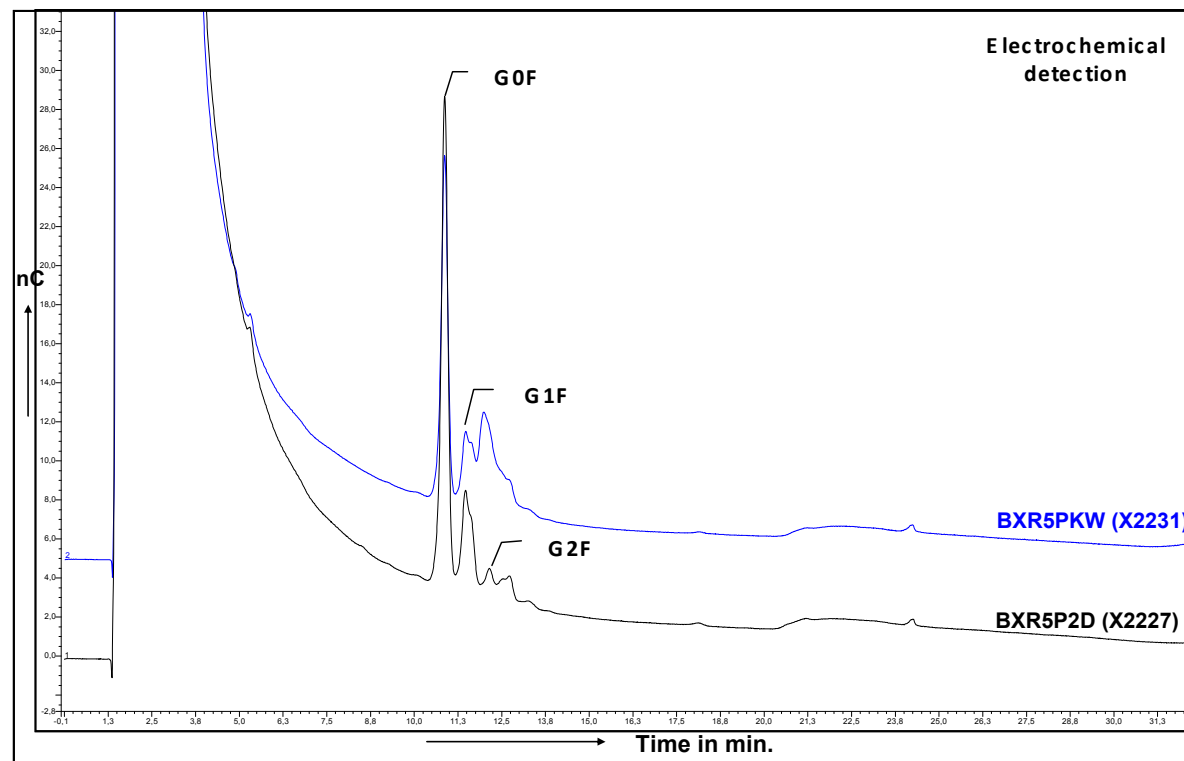
The influence of conjugation on glycan structures of BAY 1129980 was analyzed by glycan-profiling. The glycans were enzymatically released by PNGase F treatment and then analyzed by high performance liquid anion exchange chromatography using pulsed aperiometric detection. [Figure 4-4](#) shows an overlay of the BXR5PKW (ADC) and of BXR5P2D (mAb).

The antibody-drug-conjugate shows a larger peak in the G2F-region in comparison with the mAb indicating some modification by the conjugation process. [Table 4-3](#) gives the relative abundance of the individual structures.

Table 4-3. The relative abundance of the individual glycan structures of BAY 1112623 GLP-batches and BAY 1129980 (ADC) as area % are given.

Batch	Area %				
	G0	G0F	G1F	G2F	Peak 5
BAY 1112623	0.1	56.2	30.5	6.1	5.2
BXR5NHL	0.1	66.3	21.4	4.8	6.3
BXR5P2D	0.1	66.1	21.2	5.0	6.3
BXR5P2E	0.1	66.2	21.2	4.9	6.4
BXR5PKW (BAY 1129980)	n.d.	46.4	16.3	31.0	6.4

Figure 4-4. Overlay of glycan profiles from BXR5PKW (ADC) and BXR5P2D (mAb) after ion-exchange chromatography and pulsed aperiometric detection.



5. Methods Dealing with the in Vitro Biological Activity of the Molecule

5.1 Determination of the Kinetic Constants of Interaction with the Antigen

C4.4a

The basic principles of an antigen-antibody interaction are those of any bimolecular reaction. The interaction of BAY 1129980 GLP-batch BAY 1129980 and BAY 1112623 GLP-batches with its antigen was analyzed using a Biacore system. The dissociation constants were calculated from the single rate constants k_d and k_a (Table 5-1). The interaction with the antigen is in the nanomolar range. Figure 5-1 shows sensograms at different concentrations of the interaction between BAY 1129980 (BXR5PKW) and the C4.4a antigen. The ADC and the mAb practically show the same kinetic constants. The conjugation has no influence on the binding affinity to the C4.4a-antigen.

Table 5-1. Determination of kinetic constants from BAY 1129980 and BAY 1112623 GLP-batches with the antigen rh C4.4a are given.

Batch	k_a ($M^{-1} \times s^{-1}$)	k_d (s^{-1})	K (M^{-1})	K_D (M)
BAY 1112623	4.058×10^5	1.12×10^{-2}	3.61×10^7	2.77×10^{-8}
BXR5NHL	4.017×10^5	1.078×10^{-2}	3.73×10^7	2.68×10^{-8}
BXR5P2D	3.894×10^5	1.112×10^{-2}	3.50×10^7	2.86×10^{-8}
BXR5P2E	4.080×10^5	1.130×10^{-2}	3.61×10^7	2.77×10^{-8}
BXR5PKW (BAY 1129980)	3.371×10^5	1.192×10^{-2}	2.82×10^7	3.54×10^{-8}



$$k_a[Ab]x[Ag] = k_d[AbAg]$$

$$K = \frac{[AbAg]}{[Ab]x[Ag]} = \frac{k_a}{k_d} \quad K_D = \frac{k_d}{k_a}$$

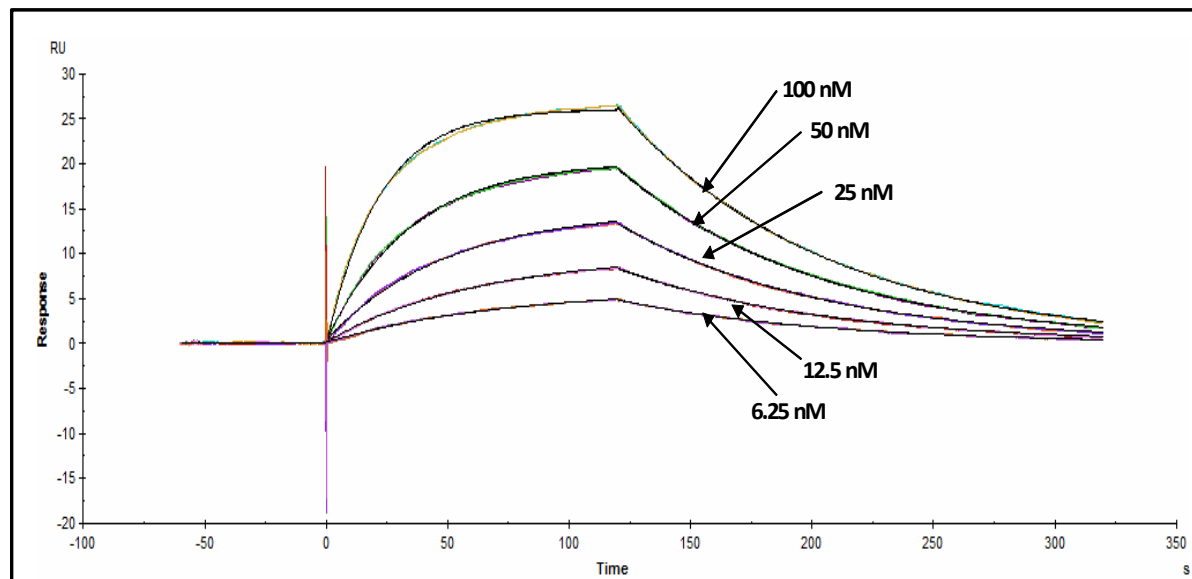
K = affinity constant M^{-1}

k_a = rate constant association $M^{-1} \times s^{-1}$

k_d = rate constant dissociation s^{-1}

K_D = dissociation constant M

Figure 5-1 Sensograms at different concentrations showing the kinetic of interaction between BAY 1129980 (BXR5PKW) and the C4.4a antigen expressed as His-tag molecule in *E.coli*.

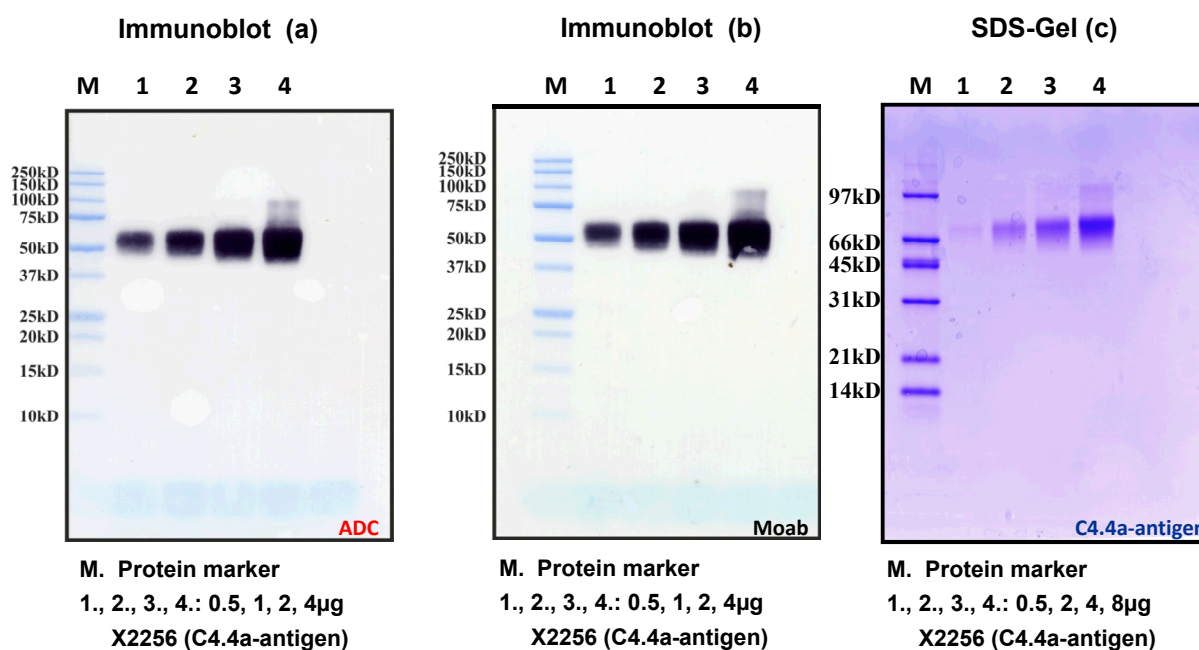


5.2 Affinity Blot of BAY 1129980 with the C4.4a Antigen

BAY 1129980 was analyzed for its affinity to the C4.4a antigen as target protein. C4.4a-antigen was expressed in HEK-293 cells as His-tag protein for better purification.

A biotinylated anti-human IgG-antibody was used as detection antibody for BAY 1129980 when it was bound. [Figure 5-2](#) a and b show the reaction of BAY 1129980 (ADC) and BXRP2D (mAb) with C4.4a-antigen under non-reducing conditions. The ADC and the mAb react in a dose dependent manner as expected with the C4.4a-antigen. [Figure 5-2](#) c shows a Coomassie blue stained SDS-gel of the C4.4a-antigen under non-reducing conditions.

Figure 5-2 12%-SDS-gel of C4.4a-antigen (X2256) was run under non-reducing conditions. The gel was blotted onto a PVDF-membrane and then reacted by C4.4a-ADC (BAY 1129980) and C4.4a-mAb (BXRP2D) and developed by a biotinylated anti-human IgG-antibody (a, b). 12%-SDS-gel of C4.4a-antigen was run under non-reducing. The gel was stained by Coomassie Blue Brilliant R-250 (c).



6. List of Abbreviations

AAA	amino acid analysis
AA	amino acid
Å	angstrom (10^{-10} m)
ACN	acetonitrile
ADC	antibody drug conjugate
Asx	asparagine or aspartic acid
6-AHA	6-aminohexanoic acid
BAY 1129980	C4.4a-ADC
BAY 1112623	anti-C4.4a monoclonal antibody
BAY 79-4682	CA9-ADC
BSA	bovine serum albumin
CAPS	cyclohexyl-3-aminopropanesulfonic acid
CHO-cell	Chinese hamster ovary cell
Cys_CM	S-Carboxymethylcysteine
CZE	capillary zone electrophoresis
2-DE	two-dimensional gel electrophoresis
D	dimensional
Da	dalton
Enz.	enzymatic
ESI-MS	electrospray ionization mass spectroscopy
Gal	galactose
GalN	glactosamine
Glu	glucose
GluN	glucosamine
Glx	glutamine or glutamic acid
Glp	pyroglutamic acid
HC	heavy chain
HPAEC	high performance anion-exchange chromatography
HPLC	high performance liquid chromatography
HRP	horse radish peroxidase
IEF	isoelectric focusing
IgG	immunoglobulin G
IPG	immobilized pH gradients
kD	kilo Dalton
LC	light chain
Man	mannose

MES	4-morpholino ethanesulfonic acid
MW	marker molecular weight
MV	mean value
m/z	mass-to-charge
nC	nano coulomb
nmol	nanomol
OD	optical density
PAD	pulsed amperometric detection
PAGE	polyacrylamide gel electrophoresis
PBS	pH 7.4 isotonic 0.01 M phosphate buffer
pI	isoelectric point
pmol	picomol
ppm	part per million
PTH	phenylthiohydantoin
PVDF	polyvinyl difluoride
RP-HPLC	reversed phase HPLC
rpm	rounds per minute
RT	room temperature
SD	standard deviation
SDS	sodium dodecyl sulphate
SDS-PAGE	sodium dodecyl sulphate polyacrylamide gel electrophoresis
SEC	size exclusion chromatography
TFA	trifluoro acetic acid